



Since January 2020 Elsevier has created a COVID-19 resource centre with free information in English and Mandarin on the novel coronavirus COVID-19. The COVID-19 resource centre is hosted on Elsevier Connect, the company's public news and information website.

Elsevier hereby grants permission to make all its COVID-19-related research that is available on the COVID-19 resource centre - including this research content - immediately available in PubMed Central and other publicly funded repositories, such as the WHO COVID database with rights for unrestricted research re-use and analyses in any form or by any means with acknowledgement of the original source. These permissions are granted for free by Elsevier for as long as the COVID-19 resource centre remains active.



A short survey of dengue protease inhibitor development in the past 6 years (2015–2020) with an emphasis on similarities between DENV and SARS-CoV-2 proteases

Sheikh Murtuja, Deepak Shilkar, Biswatrish Sarkar, Barij Nayan Sinha, Venkatesan Jayaprakash*

Department of Pharmaceutical Sciences & Technology, Birla Institute of Technology, Mesra, Ranchi 835215 (JH), India

ARTICLE INFO

Keywords:

Dengue virus
NS2B-NS3-pro inhibitors
Peptidomimetics
HTS
High-throughput virtual screening (HTVS)
Dengue-COVID-19 co-infection

ABSTRACT

Dengue remains a disease of significant concern, responsible for nearly half of all arthropod-borne disease cases across the globe. Due to the lack of potent and targeted therapeutics, palliative treatment and the adoption of preventive measures remain the only available options. Compounding the problem further, the failure of the only dengue vaccine, Dengvaxia®, also delivered a significant blow to any hopes for the treatment of dengue fever. However, the success of Human Immuno-deficiency Virus (HIV) and Hepatitis C Virus (HCV) protease inhibitors in the past have continued to encourage researchers to investigate other viral protease targets. Dengue virus (DENV) NS2B-NS3 protease is an attractive target partly due to its role in polyprotein processing and also for being the most conserved domain in the viral genome. During the early days of the COVID-19 pandemic, a few cases of Dengue-COVID 19 co-infection were reported. In this review, we compared the substrate-peptide residue preferences and the residues lining the sub-pockets of the proteases of these two viruses and analyzed the significance of this similarity. Also, we attempted to abridge the developments in anti-dengue drug discovery in the last six years (2015–2020), focusing on critical discoveries that influenced the research.

1. Introduction

Nearly 390 million people globally are at risk of developing the arthropod-borne viral disease dengue.¹ Dengue virus (DENV)² belongs to the genus flavivirus of the Flaviviridae family.³ The genus flavivirus also includes pathogenic viruses like West Nile virus (WNV), Yellow Fever virus (YFV), and Japanese Encephalitis virus (JEV).⁴ There are four distinct but closely related serotypes of dengue viruses: DENV 1, DENV 2, DENV 3, and DENV 4. Further, each serotype can be sub-classified into genotypes and strains.⁵ The virus is primarily transmitted by the arthropod vector *Aedes aegypti* and, to a lesser extent, by *Aedes albopictus*.⁶ It is responsible for varying degrees of clinical manifestations in the infected individuals, including mild flu-like symptoms to severe symptoms such as dengue hemorrhagic fever (DHF) and dengue shock syndrome (DSS). Failing to attend DHF and DSS cases

immediately can prove to be fatal.⁷ Fortunately, less than 1% of dengue patients develop DHF and DSS.⁸ Based on the incidence of DHF and DSS in the case of dengue infection, the severity of the four serotypes is found to be in the following order (DENV 2 > DENV 1 > DENV 3 > DENV 4). DENV 4 is rarely fatal.⁹ Infection with one serotype does not necessarily offer cross-immunity to other serotypes. Further, any subsequent infection can develop into severe dengue, commonly referred to as “antibody-dependent enhancement.”^{10,11} Over the years, dengue has severely affected populations in the tropical and subtropical regions of the world.¹² Some studies investigating the prevalence of dengue have identified 128 countries at risk of dengue¹³ epidemics, among which Asia alone accounts for 70% of cases. The year 2019 recorded the highest ever reported dengue cases worldwide, with Afghanistan as the new entrant, witnessing dengue infection for the first time. In the year 2020, cases were on the rise in countries like Bangladesh, Brazil, Cook

Abbreviations: DENV, Dengue virus; DHF, Dengue hemorrhagic fever; DSS, Dengue shock syndrome; HCV, Hepatitis C Virus; HIV, Human Immuno-deficiency Virus; HTS, High-throughput screening; HTVS, High-throughput virtual screening; JEV, Japanese encephalitis virus; NMR, Nuclear magnetic resonance; ORF, Open reading frames; SARS, Severe acute respiratory syndrome-coronavirus; SI, Selectivity index; SLC, Split luciferase complementation; WNV, West Nile virus; YFV, Yellow fever virus.

* Corresponding author.

E-mail address: venkatesanj@bitmesra.ac.in (V. Jayaprakash).

<https://doi.org/10.1016/j.bmc.2021.116415>

Received 30 May 2021; Received in revised form 6 August 2021; Accepted 11 September 2021

Available online 20 September 2021

0968-0896/© 2021 Elsevier Ltd. All rights reserved.

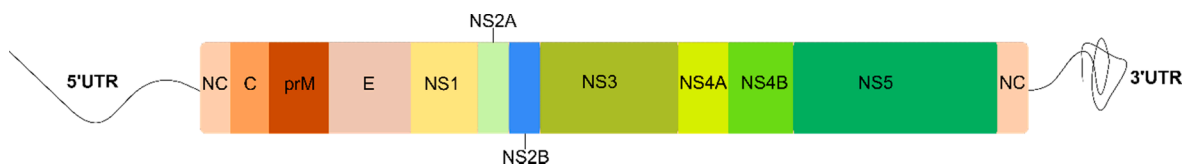


Figure 1A. Dengue virus genome.

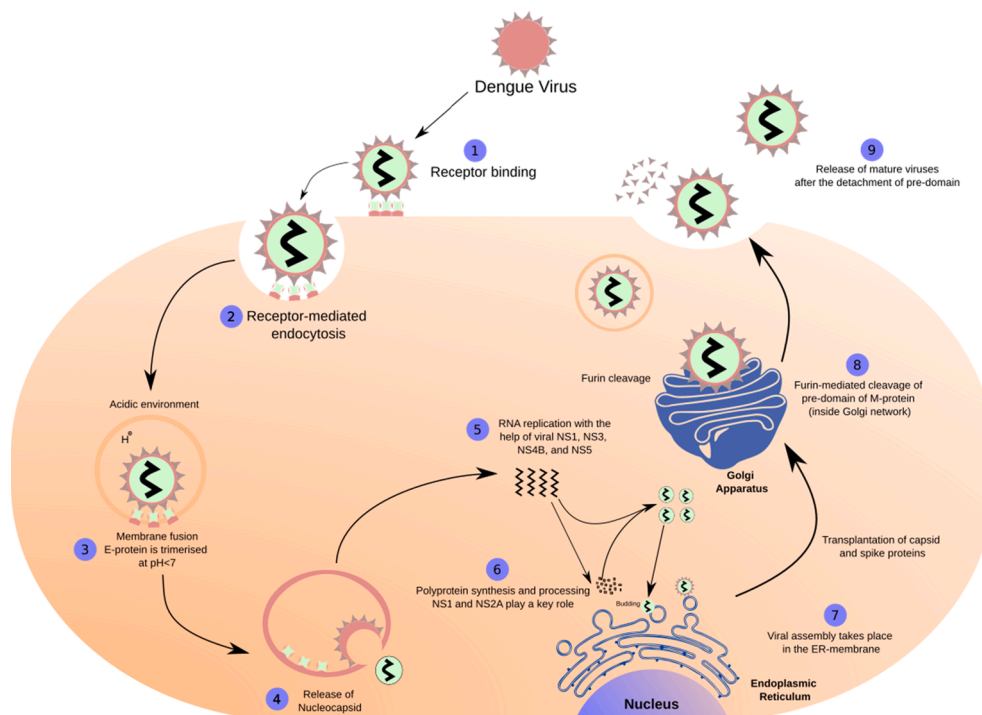


Figure 1B. The lifecycle of the Dengue virus.

Islands, Ecuador, India, Indonesia, Maldives, Mauritania, Mayotte (Fr), Nepal, Singapore, Sri Lanka, Sudan, Thailand, Timor-Leste, and Yemen.¹⁴ On the vaccine front, the current status is not highly encouraging. The currently available DENV vaccine, Dengvaxia®, launched by Sanofi Pasteur in 2015, has only been approved in 20 countries due to concerns about vaccinating seronegative patients. Seropositive and seronegative patients responded differently to the vaccine; the vaccinated seronegative patients were vulnerable to severe dengue contracting the first natural DENV infection. Currently, only individuals in the age group of 9–45 years and with at least one reported previous DENV infection are eligible for vaccination.^{14,15} Hence, these limitations aggressively demand a parallel attempt at drug development. As our group has previously published the progress made in the development of DENV protease inhibitors.¹⁶ In continuation of our previous work, in this review, along with a discussion on Dengue-COVID 19 co-infection, we have compiled the progress made in the last six years (2015–2020) toward the development of DENV protease inhibitors. We have broadly categorized our discussion into peptide inhibitors, small molecule inhibitors, inhibitors identified through a rational approach, inhibitors identified through modification of previously reported inhibitors, and drug repurposing. A section on patents and information on clinical trials has also been added. Wherever possible, we have discussed the evolution of potent molecules, reported mechanism of action of the inhibitors, and their interactions with the available crystal structures of DENV protease that demonstrated inhibitory activity. Further, the emergence of COVID-19 has stirred fresh concerns in tropical regions due to anticipated threats following a dengue co-infection. While the data on this topic is relatively premature and inconclusive, we have touched

upon Dengue-COVID-19 co-infections and outcomes in patients. This has also inspired us to draw two comparisons, one between the substrate-peptide residue preferences of DENV NS2B-NS3 protease (hereafter referred to as DENV NS2B-NS3 pro) and SARS-CoV 3CL^{Pro} and the other between various residues lining the sub-pockets of DENV NS2B-NS3 pro and SARS-CoV 3CL^{Pro}.

2. DENV genome and replication cycle

The DENV genome is approximately 11 kb long, single-stranded, positive-sense RNA, encoding a single polyprotein. The genome is processed into three structural proteins, namely, the capsid (C), envelope (E), and membrane (M) proteins and seven nonstructural proteins, i.e., NS1, NS2A, NS2B, NS3, NS4A, NS4B, and NS5 by the host proteases (Furin and signalase) and the two-component viral NS2B-NS3 protease (Figure 1A).^{17–19} The DENV NS2B-NS3 pro (serine protease), which belongs to the trypsin superfamily, contains a catalytic triad in its active site formed by His51, Asp75, and Ser135 residues.²⁰ The N-terminal domain of NS3 houses NS3 protease, which, together with 40 residues (hydrophilic) of NS2B,¹⁹ exhibits the serine protease activity.²¹ The lack of this NS2B-NS3 interaction renders the NS3 protease less active or inactive.¹⁹ Further, this NS2B-NS3 alignment forms the S₂ and S₃ sub-pockets in the protease active site.²² Since viral replication and propagation depend on the activity of DENV NS2B-NS3 pro, the complex serves as an attractive target for the antiviral drug design against DENV.²³ Figure 1B shows the basic steps involved in the replication cycle of the DENV.^{18,24,25}

Table 1
Substrate-peptide residue preferences of DENV NS2B-NS3 pro and SARS-CoV 3CL^{Pro}.

Viral proteases	Natural-cleavage sites	Non-prime site residues					Cleavage point	Prime site residues				
		P5	P4	P3	P2	P1		P1'	P2'	P3'	P4'	P5'
DENV1	NS2A-NS2B	I	W	G	R	K	Cleavage point	S	W	P	L	N
	NS2B-NS3	K	K	K	Q	R		S	G	V	L	W
	NS3-NS4A	A	A	G	R	R		S	V	S	G	D
	NS4B-NS5	G	G	G	R	R		G	T	G	A	Q
DENV2	NS2A-NS2B	T	S	K	K	R	Cleavage point	S	W	P	L	N
	NS2B-NS3	V	K	K	Q	R		A	G	V	L	W
	NS3-NS4A	A	A	G	R	K		S	L	T	L	N
	NS4B-NS5	T	N	T	R	R		G	T	G	N	I
DENV3	NS2A-NS2B	T	L	K	R	R	Cleavage point	S	W	P	L	N
	NS2B-NS3	K	Q	T	Q	R		S	G	V	L	W
	NS3-NS4A	A	A	G	R	K		S	I	A	L	D
	NS4B-NS5	G	T	G	K	R		G	T	G	S	Q
DENV4	NS2A-NS2B	G	A	S	R	R	Cleavage point	S	W	P	L	N
	NS2B-NS3	V	K	T	Q	R		S	G	A	L	W
	NS3-NS4A	A	S	G	R	K		S	I	T	L	D
	NS4B-NS5	Q	T	P	R	R		G	T	G	T	T
SARS-CoV 3CL ^{Pro}	Wild-type autocleavage sequence	S	A	V	L	Q	Cleavage point	S	G	F	R	K
	Most preferable sequence	V	C	R	L	Q		S	S	R		

3. Dengue-COVID 19 co-infection

The first case of Dengue-COVID-19 co-infection was reported by Verduyn et al. in August 2020. This has since been a significant concern in tropical areas where flaviviruses and COVID-19 infections may coexist. Since the patient showed quite severe dengue infection with no history of prior dengue infection, Verduyn et al. hypothesized that Severe acute respiratory syndrome coronavirus 2 (SARS-CoV-2) infection might have aggravated the severity of dengue. However, this contention needs further exploration as it was difficult to distinguish between the clinical features of Dengue and COVID-19. They reported that the patient showed some symptoms like prolonged fever, facial flushing skin, body-ache myalgia, arthralgia, erythema, retro-orbital eye pain, which were consistent with dengue. However, some of these overlap with the clinical features of COVID-19. Besides these, other symptoms, including thrombocytopenia and elevated liver enzymes, were also reported in both diseases.²⁶ Following this report, several other reports of co-infection have emerged across the globe. Epelbein et al. reported a case of co-infection in a traveler returning from France.²⁷ Further, Saddique et al. highlighted a case where similarity of symptoms was such that a proper distinction was only possible following a laboratory test.²⁸ These observations hint at the difficulty in distinguishing the clinical manifestation arising from the co-infection, thus highlighting the need for exploring the co-infections further.

4. DENV NS2B-NS3 pro and SARS-CoV 3CL^{Pro} substrate-peptide residue preferences

The initial efforts in the search for DENV protease inhibitors were based on the residue sequences at various cleavage sites. Further, this approach was supported by the finding that NS2B-NS3 proteases of the *Flavivirus* family have a preference for substrates having dibasic residues (Lys or Arg) at the P1 and P2 site, and further residue preference at P1' site was a small amino acid (Gly, Ala, and Ser).^{29,30} Further, Li et al. in 2005 performed functional substrate profiling of P1-P4 and P1'-P4' for all the four serotypes of DENV protease complexes using tetrapeptide and octapeptide positional scanning peptides to explore the substrate specificity of DENV NS2B-NS3 pro serotypes 1-4.³¹ Table 1 presents the outcome of their work. SARS-CoV-2, which caused the COVID-19 pandemic, belongs to the family *Coronaviridae* and genus *Betacoronoviruses*. Coronaviruses are enveloped, single-stranded, positive-sense

RNA viruses responsible for various diseases, including respiratory diseases in both animals and humans.³²⁻³⁵ The genome of SARS-CoV-2 is ~ 29.9 kb in length, and it has 14 open reading frames (ORF's) encoding for 27 proteins.³⁶ This viral genome encodes two proteases, besides Papain-like protease (PL^{Pro}), the Chymotrypsin-like cysteine protease, the 3C-like protease (3CL^{Pro}) is considered to be the main protease (also called M^{Pro}) responsible for polyprotein processing. In addition, among the coronaviruses, the sequence for 3CL^{Pro} is highly conserved.^{37,38} The fact that none of the human host cell proteases have such substrate specificity³⁹⁻⁴¹ further strengthens the rationale behind the design and development of 3CL protease inhibitors. The catalytic dyad of SARS-CoV 3CL^{Pro} is composed of Cys145 and His41, which is different from the serine protease catalytic triad (Ser-His-Asp).⁴² Here, we compared the substrate-peptide residue preferences of both DENV NS2B-NS3 pro and the SARS-CoV 3CL^{Pro} of coronaviruses. Since these two proteases have already been established as potential targets,^{23,43} it would be interesting to see the outcome of this comparison. In 2010, Chuk et al. presented the substrate-peptide residue preferences of SARS-CoV 3CL^{Pro} (Table 1). From the table, it is evident that Val > Phe > Thr residues were favored at P5 position in that order, while small hydrophobic residues like Cys and Val were more favored at P4 position, and positively charged residues with a tendency to form β -sheet structure were more favored (Arg > Val) at the P3 position. Further, at the P2 position, hydrophobic residue without β branch was most favored, and the order of residue preference was Leu > Met > Phe. Moreover, β -branch residues like Ile and Val were least preferred. At the P1 position, Gln was most favored, with Gln > His > Met as the order of preference for this position. For the prime side residue preferences, P1' favored small residues; the order of preference was Ser > Ala > Cys > Gly. The P2' and P3' positions did not exhibit any specific residue preferences; however, it was observed that small residues like Ser, Gly, and Ala were more prone to cleavage by the protease than the larger residues. It was also observed that solvent-exposed sites like P5, P3, and P3' favored positively charged residues suggesting that the electrostatic interactions being responsible for the catalytic activity of the 3CL^{Pro}. The P1 site was most selective as cleavage was only observed in the presence of Gln, Met, or His. Substituting all the favored residue on positions P5 to P1 resulted in a 2.8 fold higher activity than the wild-type substrate sequence.⁴⁴ Table 1 shows the substrate-peptide residue preferences of DENV 1-4 NS2B-NS3pro and the SARS-CoV 3CL^{Pro}.^{31,44} In summary, substrate residue specificity of DENV NS2B-NS3 pro is mainly seen for the P2-P1-P1'

Table 2
Residue lining the sub-pockets of DENV NS2B-NS3 pro and SARS-CoV-2 3CL^{pro}.

Viral protease	Sub-pocket residues				
	S4	S3	S2	S1	S1'
DENV NS2B-NS3 pro	Val154	Leu128	<i>Gln35</i>	Tyr150	Ile36
	Val155	<i>Asp129</i>	Asn152	<i>Leu115/Thr/Ile</i>	His51
	Gly153	Pro132	<i>His51</i>	<i>Ser163</i>	Ser135
		Val155	<i>Asp75</i>	Ile165	Gly151
		<i>Arg157/Lys/Thr</i>			
SARS-CoV-2 3CL ^{pro}	<i>Asp187</i>	His41, His164	<i>Gln189</i>	His163, His164, His172	Cys 145
	Met165	Met49, Met165	<i>Arg188</i>	Phe140	
	Glu166	<i>Asp187</i>	Met49	Met165	
	Leu167	<i>Arg188</i>	Cys144, Cys145	<i>Glu166</i>	
	Pro168	Tyr54	<i>His41</i>	<i>Leu141</i>	
	Gln192		Thr26, Thr25	Cys145	
	Thr190		Leu27	<i>Ser144</i>	
	<i>Arg188</i>		Gly143		

Note: Residues with similar color share properties by virtue of their side chains.

regions. While P2–P1 had dibasic residue preference (Lys, Arg, except for Gln as P2 residue at the NS2B/NS3 cleavage point in DENV 1–4 pro), the P1' region had a preference for smaller sized residues (Ser, Gly). In the case of SARS-CoV 3CL^{pro}, specificity was seen for P2, P1, and P1' region,⁴⁵ where it was observed that Gln was indispensable for the P1 site. Leu was favored most at P2 site, and similar to DENV^{pro}, Ser was favored at P1.'

5. Residues lining the sub-pockets of DENV pro and SARS-CoV 3CL pro

As mentioned above, the substrate specificities for both the proteases have been well defined. In this section, the corresponding sub-pocket occupancies of the residues involved have been discussed. Table 2 summarizes the residues lining the corresponding S4, S3, S2, S1, and S1' pockets of both DENV^{pro}³¹ and SARS-CoV-2 3CL^{pro}.^{46–49} The overlap of residues within the pockets is due to the common wall between the pockets. It is evident from the comparison that there is no exact overlap of residues lining the sub-pockets of both the proteases, except for Ser and Leu in the S1 pocket, Gln and His in the S2 pocket, and Arg and Asp in the S3 pocket. However, although the residues are different, residues with similar properties overlap the sub-pockets of both the proteases. The S1 sub-pocket residues (Tyr, Leu, Ile, Phe, and Met) lining both the proteases have hydrophobic side chains. Similarly, in the S2 pocket, residues (Arg, His) from both the proteases have positively charged basic side chains. In addition, residues with polar uncharged side chains (Gln, Asn, and Thr) line both the proteases. In the S3 sub-pocket, residues (Leu, Val, Met, and Tyr) lining both the proteases have hydrophobic side chains. It can also be seen that residues with positively charged basic side chains (Arg, Lys, and His) constitute the sub-pockets. Finally, the S4 sub-pocket of both the proteases are lined by residues with hydrophobic

side chains (Val, Met, and Leu). Besides this, residues like Cys, Pro, and Gly lining different sub-pockets of both the proteases have tendencies to form various interactions, including hydrogen bond and hydrophobic interactions. While much needs to be explored before arriving at a conclusion, we believe that this similarity could be exploited in the future for developing dual inhibitors against both proteases.

6. Design and discovery of DENV NS2B-NS3 pro inhibitors

This section summarizes the research on inhibitors reported in the last six years (2015–20) and summarizes the predicted interactions of a few key residues. Most interactions were common among reported peptide inhibitors. Inhibitors other than peptides were also critically examined for their predicted interactions with the proteases. Besides, any common attributes from different chemical structures were also examined. Since we have already compared the substrate-peptide residue preferences and residues lining the proteases for DENV and SARS-CoV-2 in the aforementioned sections, the insights provided below could guide the development of potent dual inhibitors. However, experimental validations remain an ultimate tool for any in-silico favored results.

6.1. Peptide inhibitors

Anti-DENV drug development began with the design of substrate-based peptide inhibitors against DENV NS2B-NS3 pro. However, the relatively flat topography of the DENV protease active site posed numerous challenges in drug design.²² In addition, there was a significant possibility of developing compounds with compromised pharmacokinetic properties as the non-prime side favored positively charged residues which would ultimately impart a negative charge to the active site. Despite these apprehensions, attempts were made to design peptide

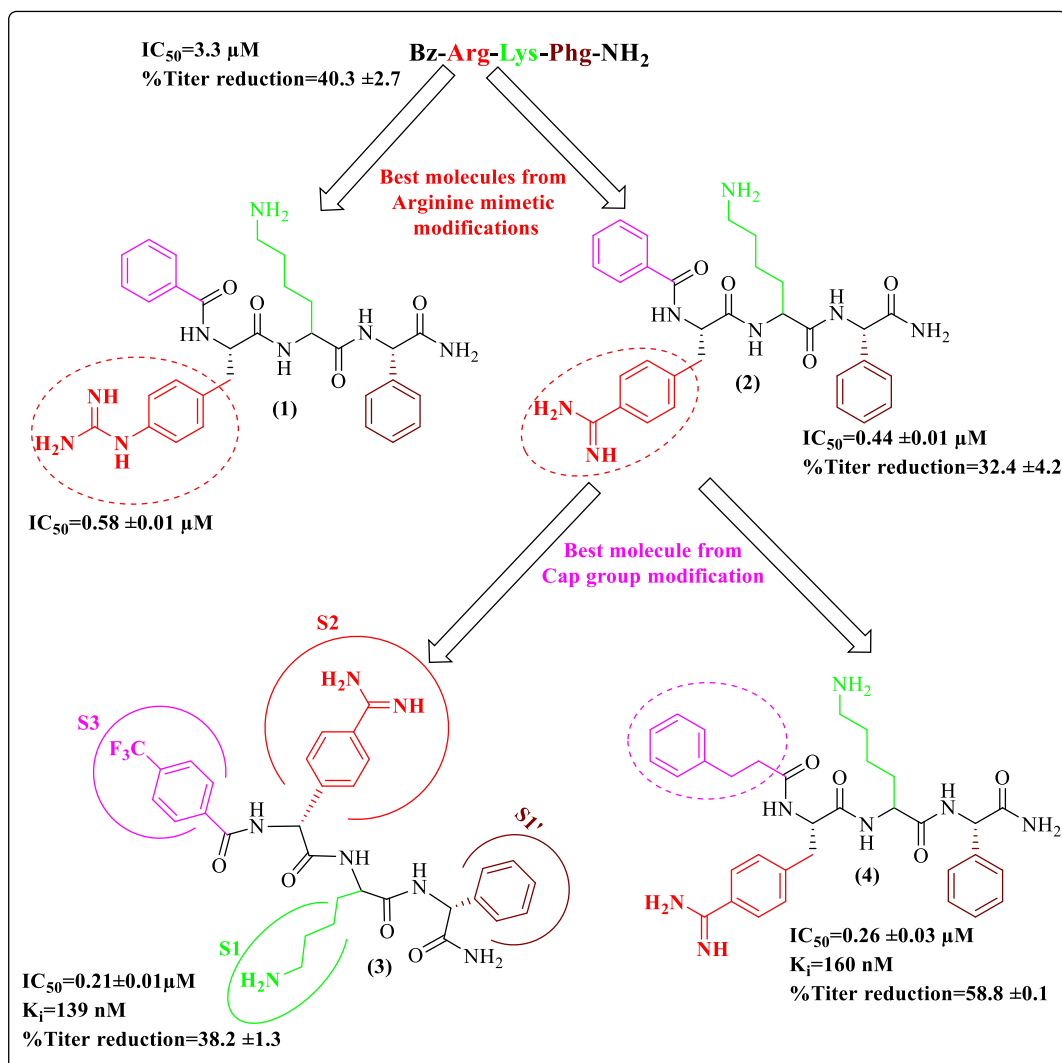


Figure 2. Weigel et al. (2015) tripeptide modification & predicted occupancy of the inhibitor (3) at subsites of protease.

inhibitors and peptidomimetics. Eventually, inhibitors with nanomolar affinities were obtained. The peptide inhibitors reported in the last six years have been discussed in the subsections, namely substrate-peptide analogs of non-prime side, peptide conjugates, and cyclic peptides.

6.1.1. Substrate-peptide analogs of non-prime side and Substrate-peptide conjugate from common tripeptide (Cap-Arg-Lys-Phe-NH₂)

In this section, we discuss three inhibitors developed by modifying a common tripeptide with varying cap (Cap-Arg-Lys-Phe-NH₂) reported by Behnam et al.⁵⁰ The first modification was done by Weigel et al.. They observed that previous modifications of peptide hybrids did not optimize the S₂ pocket, considering the target affinity.^{50–52} Hence, arginine mimetic moieties were screened to find a suitable fit. This work revolved around already established tripeptide Bz-Arg-Lys-Phe-NH₂.⁵⁰ They synthesized and performed in-vitro characterization of potent peptidic inhibitors of DENV pro by incorporating phenylalanine and phenylglycine derivatives as arginine-mimicking groups. Figure 2 shows the best two analogs, *N*-Benzoyl-capped tripeptides having (4-guanidino)-*L*-phenylalanine (1) and benzamidine (2) as arginine mimetic modification with inhibitory concentrations in the sub-micromolar range. Further, the cap modifications yielded the most promising compound 3 (Figure 2) with an IC₅₀ value of 0.21 μM and a K_i value of 139 nM. Antiviral activity of the best molecules and the reference compound (Bz-Arg-Lys-Phe-NH₂) on Huh-7 cell line infected with DENV2 serotype

showed a 58% reduction of viral titer for compound 4, which was highest in the series (Figure 2). However, PAMPA studies discouraged further development due to poor membrane permeability of the 15 synthesized tripeptides, possibly due to the presence residues at P1 and P2 position having positively charged side chains amounting to high polarity; this was also considered the reason for low antiviral activity. Molecular docking studies of compound 3 (Figure 2) against protease (PDB 3U11) predicted that the basic residue of arginine mimetic analog occupied the S₂ pocket and appeared to be involved in electrostatic interaction with Asp75 also other occupancies could be seen in the figure.⁵³

The second modification-based study in this series was conducted by Behnam et al. (2015), who developed substrate-based peptide inhibitors and extended their work toward the development of potential dual inhibitors of DENV and WNV pro by synthesizing and performing an extensive biological evaluation of inhibitors containing benzyl ethers of 4-hydroxyphenylglycine as non-natural peptidic building blocks. Figure 3 outlines the critical inhibitors from their work and displays the best compound obtained at each modification step. Their work was centered around *retro*-peptide sequences (Bz-Arg-Lys-Nle-NH₂), having good inhibitory activity against DENV2 pro.⁵¹ The replacement of Nle with Phe (Bz-Arg-Lys-*L*-Phe-NH₂, IC₅₀ = 3.32 μM) improved the inhibition profile.⁵⁰ Thus, the same molecule used by Weigel et al. was optimized here in a three-step protocol, involving optimization of this

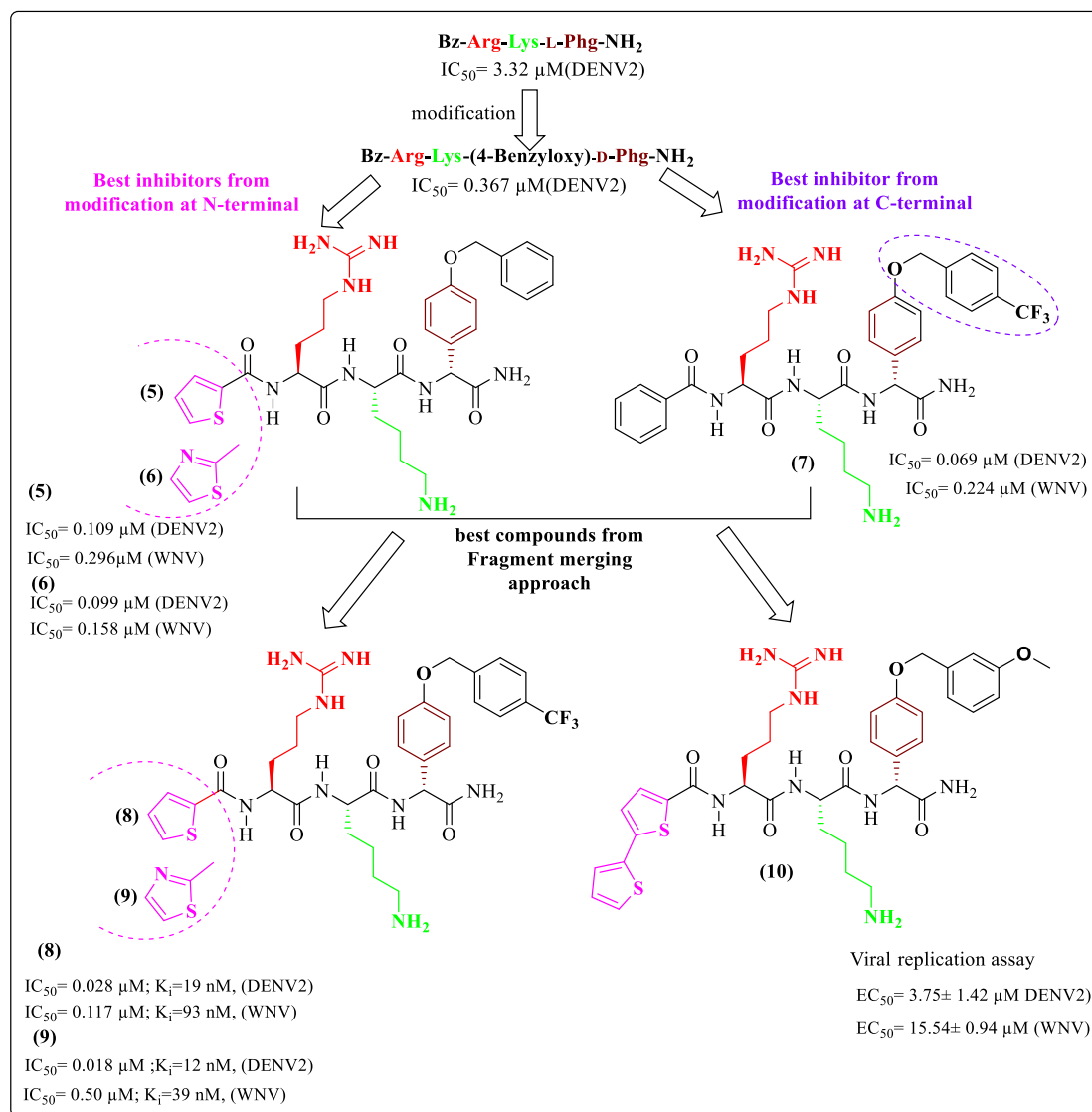


Figure 3. Behnam et al. (2015) modifications.

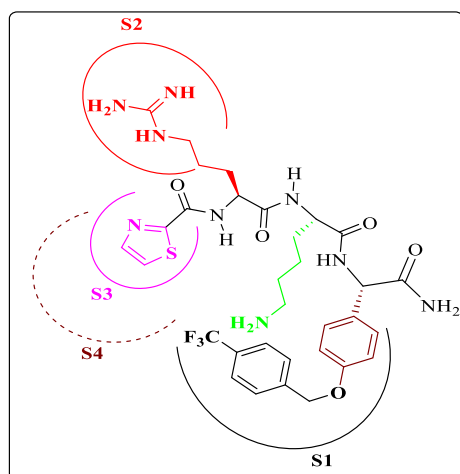


Figure 4. Predicted pocket interaction of inhibitor (9) within DENV2 NS2B NS3 pro.

sequence which ultimately settled with modifying the C-terminal 4-hydroxyphenylglycine of the tripeptide to the benzyloxy ether (Bz-Arg-Lys-(4-benzyloxy)-D-Phg-NH₂) and having an IC₅₀ value of 0.367 μM. Further, simultaneous C & N-terminal modification of the optimized sequence was performed, and N-terminal modification led to various caps being optimized to yield dual inhibitors with nanomolar inhibition. Finally, a few caps (with thiophene ring and thiazole ring) showed favorable results, and resulting compounds 5 and 6 (Figure 3) had an IC₅₀ value of 109 nM and 99 nM respectively against DENV2 pro. The C-terminal optimization generated Bz-Arg-Lys-(4-CF₃-benzyl ether)-D-Phg-NH₂, (7, Figure 3) with an IC₅₀ of 0.069 μM. The final fragment merging yielded compounds 8 and 9 (Figure 3) with K_i values of 19 nM and 12 nM, respectively, against DENV2 pro. Several of these newly discovered protease inhibitors significantly reduced dengue and WNV titers in cell-based assays of virus replication. The most active analog, compound 10 (Figure 3), showed an EC₅₀ value of 3.4 μM against DENV-2 and 15.5 μM against WNV. In general, the compounds showed less inhibition in WNV, suggesting a subtle difference in active sites of DENV and WNV proteases. Once again, PAMPA studies revealed weak permeability, possibly due to the same reason. Docking studies of tripeptides against DENV3 pro (PDB 3U11) showed that the tripeptides assumed a near cyclic confirmation inside the binding site of the protease. Figure 4 shows the predicted occupancy of different pockets by

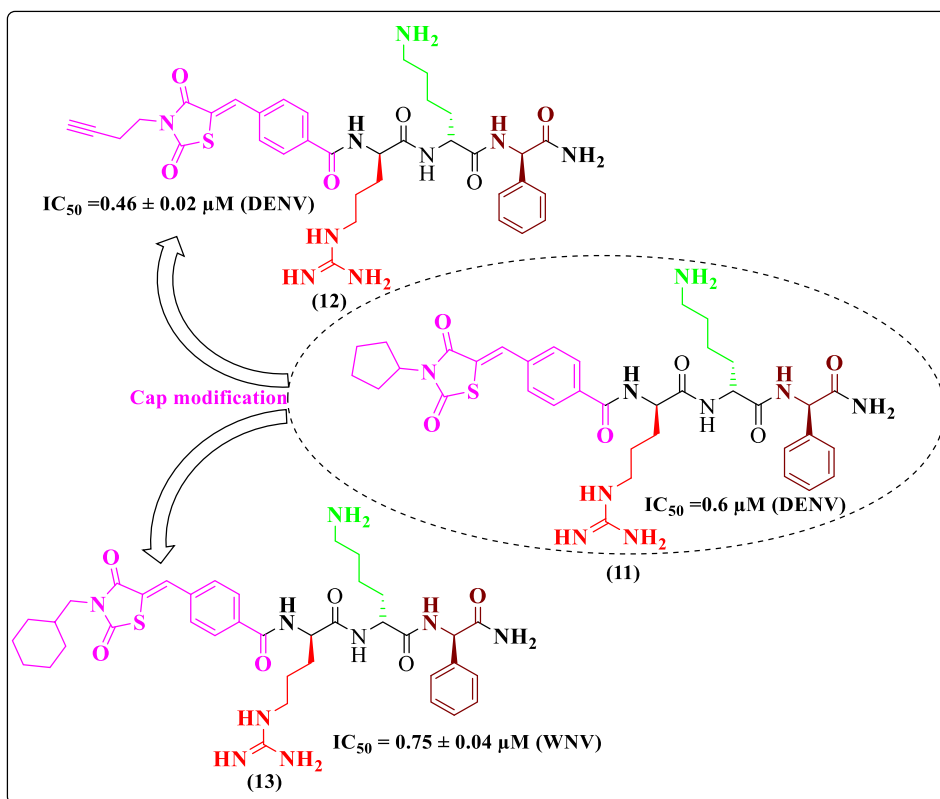


Figure 5. Bastos et al. (2015) modifications.

Table 3

Compounds arising from tripeptide modification and their predicted pocket occupancies.

Tripeptide for modification ⁵⁰	Potent compounds	IC ₅₀ (μM)	
Cap-Arg-Lys-Phg-NH ₂	Compound 3	IC ₅₀ = 0.21 μM	
	Compound 9	IC ₅₀ = 0.018 μM	
	Compound 12	IC ₅₀ = 0.46 ± 0.02 μM	
Residues of inhibitor	Predicted pocket occupancies		
	Compound 3*	Compound 9 [#]	Compound 12
Phg/Phg modification [#]	S ₁ '	S ₁	S ₁
Arg/Arg-mimetic*	S ₂	S ₂	S ₂
Lys	S ₁	S ₁ , S ₃ , S ₄	S ₁ , S ₂
Cap group (varying)	S ₃	S ₃ , S ₄	S ₃ , S ₄

inhibitor 9. The occupancy was similar to that of the previous inhibitor and an identified, predicted key interaction was that of Alkyl side chain residue Val155 which exhibited a π - σ interaction with the phenyl ring of ether.⁵⁴

Sometimes, peptides are conjugated with small molecules for improved inhibitory activity against the targeted enzyme. One such attempt was made by Bastos et al. in 2015 while searching for a dual inhibitor against DENV and WNV NS2B-NS3 protease. They modified a molecule similar to that developed by Behnam et al. with a varying cap group.⁵⁰ Thus, the third attempt to modify tripeptides led to the modification of compound 11, giving rise to compounds 12, 13 (Figure 5), which turned out to be potent inhibitors of DENV NS2B-NS3 pro (IC₅₀ = 0.46 ± 0.02 μM) and WNV pro (0.75 ± 0.04 μM), respectively. The K_i value of compound 12 was found to be 0.40 ± 0.03 μM. The docking of compound 12 against DENV pro predicted the occupancy of phenylglycine in the S₁ pocket and arginine in the S₂ pocket. The cap occupied the S₃ and S₄ pockets, and lysine was positioned between S₁ and S₂

pockets. The results showed four hydrogen bonding and twelve nonbonding interactions, besides this one of the predicted key interactions involved residue, Tyr215, engaged in a π - π stacking interaction⁵⁵.

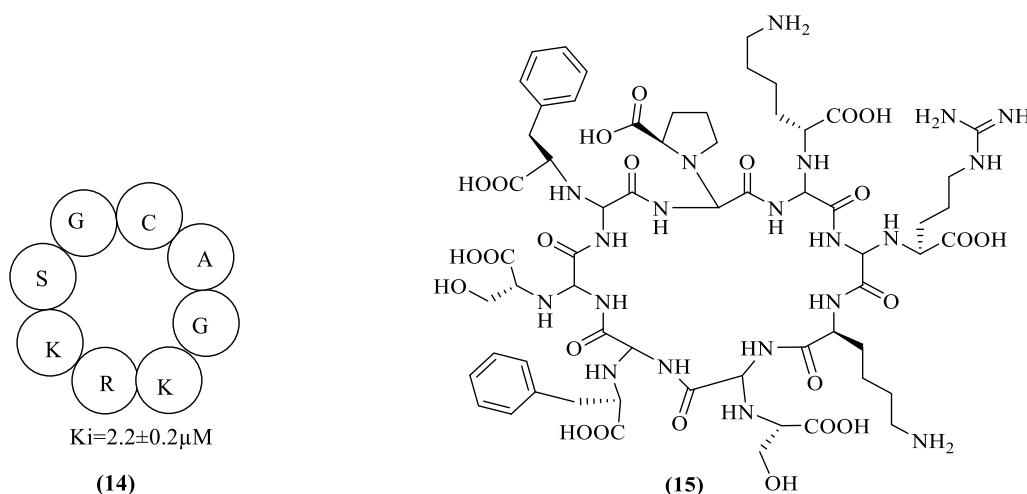
The common observation about the occupancies of the residues of the potent molecules in different pockets is shown in Table 3. It can be seen that they have almost a common pattern of occupancy. Arginine mimetic modification of Weigel et al. however, influences the position of Phg wherein it gets displaced to the S₁' pocket. The best inhibition (IC₅₀ = 0.018 μM) of protease was witnessed when Phg occupied the S₁ pocket. This tripeptide was so far, the best reported protease inhibitor identified. However, as with previous cases, pharmacokinetic challenges remained a major concern, for which the probable solutions have been discussed later on in this review.

6.1.1.1. Cyclic peptides against DENV NS2B-NS3 pro. The peptides discussed above targeted the non-prime side and had their own merits and demerits. Lin et al. (2017) observed that the currently available designs focused on the non-prime side of the DENV protease active site and almost always led to low lipophilic and nonspecific scaffolds. This prompted them to exploit the advantages of aprotinin (58 amino acids protein) for designing new cyclic peptides as aprotinin showed a high affinity for DENV2 pro (K_i = 26.9 nM). Their strategy of designing new cyclopeptides was based on the structure of aprotinin targeting the active site pockets S₃-S₄' of the DENV pro. After analyzing aprotinin's binding loop, they found that the prime side significantly modulated DENV pro binding affinity.⁵⁶ Their designed cyclic peptides showed interaction with both sides of the active site. The design was based on the two loops of aprotinin, linked together with a glycine linker. The first loop, called the binding loop, was significant in binding to DENV pro, while the second loop was incorporated into the design to maintain binding loop structure and rigidity. Also, their previous work identified the key factors affecting binding affinity, which were hydrogen bonding contributed by P1 and P2' residues, the P3' and P4' residue hydrophobic

Table 4

Lin et al. (2017) modifications and the resulting inhibition constants of various cyclic peptides. # Peptide bond, *Disulphide bond, Bz: Benzoyl capping.

Cyclic peptides	(12–18) Binding loop residues (aprotinin)							Glycine Linker		(35–39) Aprotinin's second loop residues					K _i (μM)
	P3	P2	P1	P1'	P2'	P3'	P4'			35	36	37	38	39	
Length optimization															
1.	Pro	Cys*	Lys	Ala	Arg	Ile	Ile	Gly	Gly	Tyr	Gly	Gly	Cys*	Arg	232.3 ± 69.9
2.	Pro	Cys*	Lys	Ala	Arg	Ile	Ile	Gly	Gly	Tyr	Gly	Gly	Cys*	Ala	678.3 ± 244.1
3.	Pro	Cys*	Lys	Ala	Arg	Ile	–	Gly	–	Tyr	Gly	Gly	Cys*	Ala	376.8 ± 204.1
4.	Pro	Cys*	Arg	Ala	Arg	Ile	–	–	–	Tyr	Gly	Gly	Cys*	Ala	966.1 ± 328.8
5.	Pro	Cys*	Lys	Ala	Arg	Ile	–	–	–	Tyr	Gly	Gly	Cys*	Ala	14.5 ± 6.7
6.	Pro	Cys*	Arg	Ala	Arg	Ile[#]	–	–	–	Tyr[#]	Gly	Gly	Cys*	Ala	2.9 ± 0.8
7.	Pro	Cys*	Arg	Ala	Arg	Ile	–	–	–	Tyr	–	Gly	Cys*	Ala	467.9 ± 68.7
8.	Pro	Cys*	Arg	Ala	Arg	Ile	–	–	–	–	Gly	Gly	Cys*	Ala	780.3 ± 195.5
9.	Pro	Cys*	Arg	Ala	Arg	Ile	–	–	–	–	Gly	Gly	Cys*	Arg	29.7 ± 5.8
10.	–	Cys*	Arg	Ala	Arg	Ile	–	–	–	Tyr	Gly	Gly	Cys*	Arg	145.1 ± 27.9
11.	Pro	Cys*	Arg	Ala	Arg	Ile	–	–	–	–	–	Gly	Cys*	Ala	101.2 ± 24.8
Sequence optimization															
12.	Pro	Cys*	Arg	Ala	Arg	Ile[#]	–	–	–	Tyr[#]	Gly	Gly	Cys*	Ala	2.9 ± 0.8
13.	Bz	Cys*	Arg	Ala	Arg	Ile	–	–	–	Tyr	Gly	Gly	Cys*	Ala	33.2 ± 6.5
14.	Pro	Cys*	Arg	Ala	Gln	Ile	–	–	–	Tyr	Gly	Gly	Cys*	Ala	No Binding
15.	Pro	Cys*	Arg	Ala	Trp	Ile	–	–	–	Tyr	Gly	Gly	Cys*	Arg	19.7 ± 8.8
16.	Pro	Cys*	Arg	Ala	Trp	Ile	–	–	–	Tyr	Gly	Gly	Cys*	Ala	144.8 ± 54.4
17.	Pro	Cys*	Arg	Ala	Arg	Ile	–	–	–	Asp	Gly	Gly	Cys*	Ala	69.3 ± 24.4
18.	Pro	Cys*	Arg	Val	Arg	Ile	–	–	–	Asp	Gly	Gly	Cys*	Ala	35.8 ± 16.4
19.	Pro	Cys*	Arg	Val	Arg	Ile	–	–	–	Tyr	Gly	Gly	Cys*	Ala	25.6 ± 9.9

**Figure 6.** Cyclic peptides of Xu et al. (14) & Takaji et al. (15).

packing, and maintaining the aprotinin binding loop conformation intact in the designed cyclic peptide.⁵⁶ Analogous to the structure of aprotinin, there was a need to optimize the binding loop from residue 12 to 18 (Pro13 to Ile18/Ile19) of aprotinin, the linker between the binding loop, and the second loop of aprotinin spanning from residue 35 to 39 (Tyr35/Gly36 to Arg39) in the newly designed cyclopeptides. Also, the linker glycine residues were either retained or were omitted entirely between Ile18/Ile19 and Tyr35/Gly36. Aprotinin's disulfide bond was retained by keeping a disulfide bond between Cys14 of the first loop and Cys38 of the second loop. The length of the binding loop was optimized and compounds with and without linker (one or two Gly residues) were observed, the length of the second loop was optimized and eventually these modifications yielded cyclic peptides of varying lengths. Also, the preferences of different residues at a different position were understood and correlated with the obtained K_i values. The best inhibitor showed a K_i value of 2.9 μM against wild-type DENV3 pro. Also, the preference of residues for the P1 and P2' positions was established. The key finding from this effort was that the preference between two basic amino acids Lys and Arg, was context-dependent at P1, and Arg was favored at P2' position as it appeared to have more interactions with other residues through hydrogen bonding and van der Waal forces. The choice of

optimal C-terminal residue was dependent on the length of the cyclic peptide since different lengths favored different residues at the C-terminal. However, in the native aprotinin, Arg39 was replaced with alanine. The flexibility was limited to alanine in most of the derivatives, and results were based on binding interactions. Similarly, the significance of P3 residue (N-terminal) was analyzed, and it was found that proline was more favored than a benzoyl cap at this position. However, the presence of proline was found to be context-dependent in the entire experiment as the removal of proline in some cyclic peptides did not change the activity significantly. Table 4 shows the binding affinity of cyclic peptides resulting from the incorporated changes in the optimization process. Although the most effective cyclic peptide obtained had a K_i value of 2.9 μM against wild-type DENV3 pro, this value was quite high when compared to the aprotinin inhibition constant of 29 nM against DENV2 pro. Hence, few strategies including, making the molecule more rigid and less bulky, improving the permeability and substituting cleavable peptide bonds between P1 and P1' with non-cleavable bonds to ensure cyclic structure intact were recommended and further it was predicted that any combination of these set of changes could yield a more rigid molecule with good binding affinity.⁵⁷

Although nearly all the parameters were incorporated for

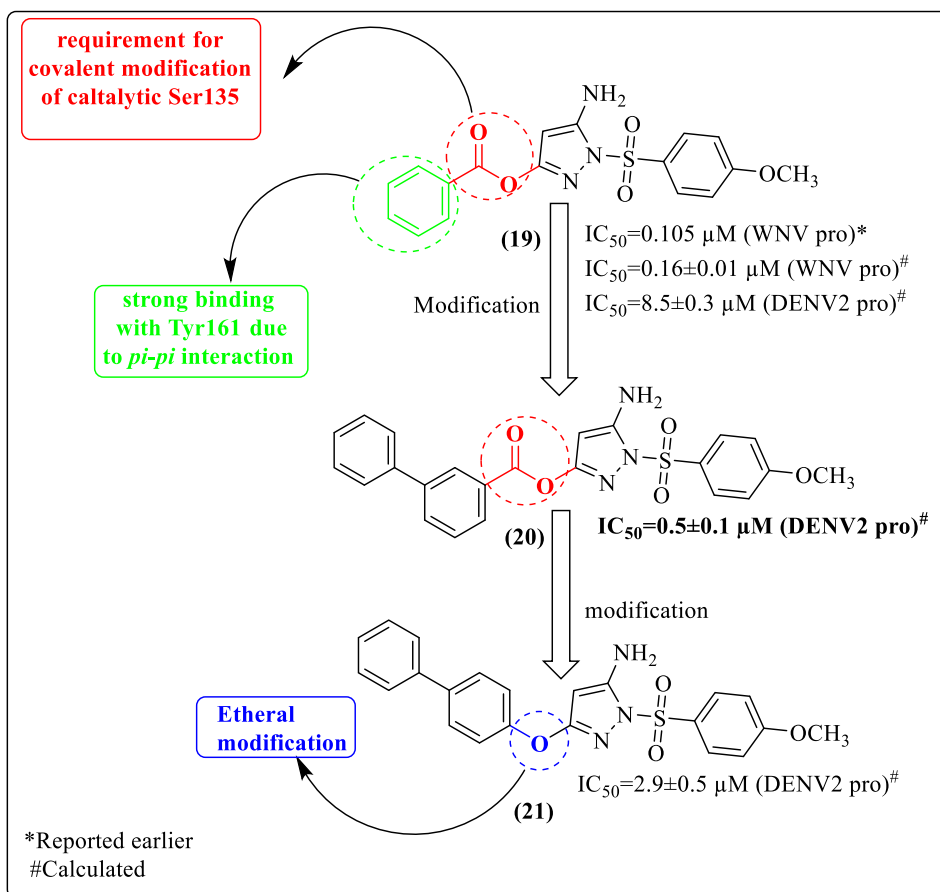


Figure 7. Koh et al. (2015), structure-guided small molecule optimization.

optimization in the above study, the results were not significantly encouraging. It was suggested that reducing the molecule's flexibility could provide a more potent inhibitor as high flexibility was previously attributed to the low protease inhibition. In addition to improving the protease inhibitory profile, it is also essential to optimize the compound for antiviral activity. However, studies in the past made no such attempts. Takagi et al. (2017) synthesized 33 cyclic peptides, and for the first time, identified a novel cyclic peptide inhibitor with antiviral activity. Their work began with the modification of the lead compound from Xu et al. (eight-residue cyclic peptide, 14) (Figure 6). After alanine scanning and studying the model by Xu et al., they learned that P1-Lys, P3-Lys, P2-Arg interactions were essential for the activity and, therefore, were retained in the new design. Also, since the environment around P1', P2', and P4' residues appeared hydrophobic, it was also believed that these positions could be substituted with hydrophobic groups and could result in hydrophobic interactions between the inhibitor and the enzyme. After optimizing the P1', P2', and P4' positions, they established that at P1'-Ser was indispensable and P2'-Gly replacement with the hydrophobic group was valuable. It was also revealed that preferential replacement at this position was in the following order: L-homophenylalanine > L-phenylglycine > L-phenylalanine = D-homophenylalanine. Further, P4' was fixed with D-phenylalanine. P3'-Ser yielded satisfactory results compared to P3'-Ala. However, the best protease inhibitory activity was observed when, D-proline replaced the flexible P4-Gly. The best cyclic peptide 15 (Figure 6) had an IC_{50} value of 0.95 μM . Docking study of this molecule using DENV2 pro, attributed good protease inhibition to the β -turn like conformation of the cyclic peptide inside the protease. Markedly, Compound 15 was not an as effective antiviral agent as intended. The high hydrophilicity due to the side chains of the residues would have inhibited the membrane permeability of the cyclopeptide. Significant efforts were made to

improve its permeability^{58,59} while maintaining protease inhibition and antiviral efficiency. In the process, 11 cyclic peptides obtained were further subjected to antiviral assay. Finally, the optimization efforts yielded a cyclopeptide (P4' D-Arg, P3' L-Arg, P2' L-Lys, P1' L-Lys, P1 D-2NaI, P2 L-hPhe, P3 L-Phe, and P4 D-NaI), which showed promising antiviral activity with an EC_{50} value of 2.2 μM without significantly compromising the IC_{50} value (1.1 μM).⁶⁰ The cyclic peptide was designed keeping the substrate-peptide residue preferences into consideration. The aromatic residues, introduced into the design improved the activity. Notably, the permeability issues were addressed without compromising the protease activity. Such attempts viz. introduction of amphipathic sequence motifs and the proper combination of arginine and hydrophobic aromatic residues could be applied to future cyclic molecules to improve the permeability issues and eventually obtain the desired potent antiviral agent.

6.2. Small molecule inhibitors

Small molecules offer significant advantages over large peptides in terms of complexity, feasibility, and scalability. Small molecule inhibitors can introduce large conformational changes in DENV NS2B-NS3 pro.⁶¹ This section describes various attempts to develop non-peptide small molecule inhibitors. These have been sub-classified into inhibitors from structure-guided small molecule optimization, from natural sources, from High-throughput screening (HTS), HTVS, and a rational design approach. Further, in these subsections, the chemical class is also mentioned. In this section, we discuss various efforts made toward optimizing the potential inhibitors by recognizing the scaffolds involved in the protease inhibitory activity as well as gaining knowledge about protease residues predicted to be involved in the interaction with the inhibitor.

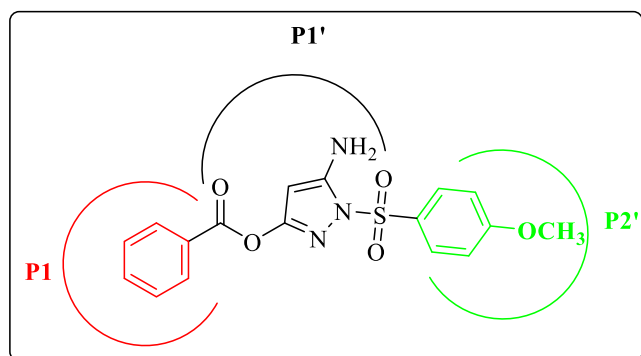


Figure 8. Predicted occupancy of the inhibitor (19) at different DENV protease sites.

6.2.1. Inhibitor from structure-guided small molecule optimization (pyrazole ester derivative)

Koh et al. used a potent WNV protease inhibitor (**19**, Figure 7, IC_{50} = 0.105 μ M), a pyrazole ester derivative for DENV pro drug development. The compound was previously identified by Johnston et al. by performing HTS using the National Institute of Health compound library containing > 65,000 compounds.⁶² The structure-guided small molecule optimization effort improved compound potency and selectivity for DENV protease. Figure 7 shows how the modifications affected the IC_{50} values of compound **20** (IC_{50} = 0.5 ± 0.1 μ M) and **21** (IC_{50} = 2.9 ± 0.5 μ M). Protease inhibitor binding interactions were confirmed biophysically using nuclear magnetic resonance (NMR). The molecular weight of DENV2 pro treated with compound **19** and DENV pro in control (DMSO solution) by ESI-TOF MS indicated benzoylation of DENV2 pro by inhibitor. Finally, the group confirmed a covalent

interaction between catalytic triad serine and inhibitor **19**, as no change in molecular weight was observed when inhibitor **19** was treated with mutant DENV2 pro, which had Ala in place of Ser135 in the NS3 domain. The inhibitor appeared to have been occupying the active site. NMR analysis provided an insight into the protease inhibitor binding interactions. Further, they explored protease inhibitor molecular interaction by titrating inhibitor **19** against DENV2 pro. The chemical shift perturbation findings were in agreement with ESI-TOF MS results.

Further, molecular docking of inhibitor **19** against DENV3 pro (PDB 3U1I) predicted the occupancy of inhibitor at different sites (Figure 8). Also, a few other interactions were predicted, including van der Waals and hydrogen bonding. Few interactions and positionings involved the identified key residues (Pro132 and Tyr161), the ester phenyl group occupied the P1 site, and the phenyl group appeared to be trapped between Pro132 and Tyr161, and a π - π interaction was predicted between the ester phenyl group and Tyr161. This work strongly suggested that this class of compounds inhibited flavivirus protease through targeted covalent modification of active site serine.⁶³

6.2.2. Inhibitors from natural sources

6.2.2.1. Flavonoids, polyphenolic metabolites (PCA) and flavanones.

Over the years, many natural sources have been explored for DENV pro inhibition. Encouraged by the role of bioflavonoids, flavonoids, and chalcone derivatives in DENV pro inhibition and newly identified allosteric sites in the DENV2 pro responsible for non-competitive inhibition,⁶⁴⁻⁶⁶ De Souse et al. (2015) evaluated six flavonoids (Agathisflavone, quercitrin, and isoquercitrin isolated from a natural source and three purchased from a commercial source) against DENV2 and DENV3 NS2B-NS3 pro. Agathisflavone (**22**, Figure 9) emerged as the best non-competitive inhibitor of both the proteases with IC_{50} values

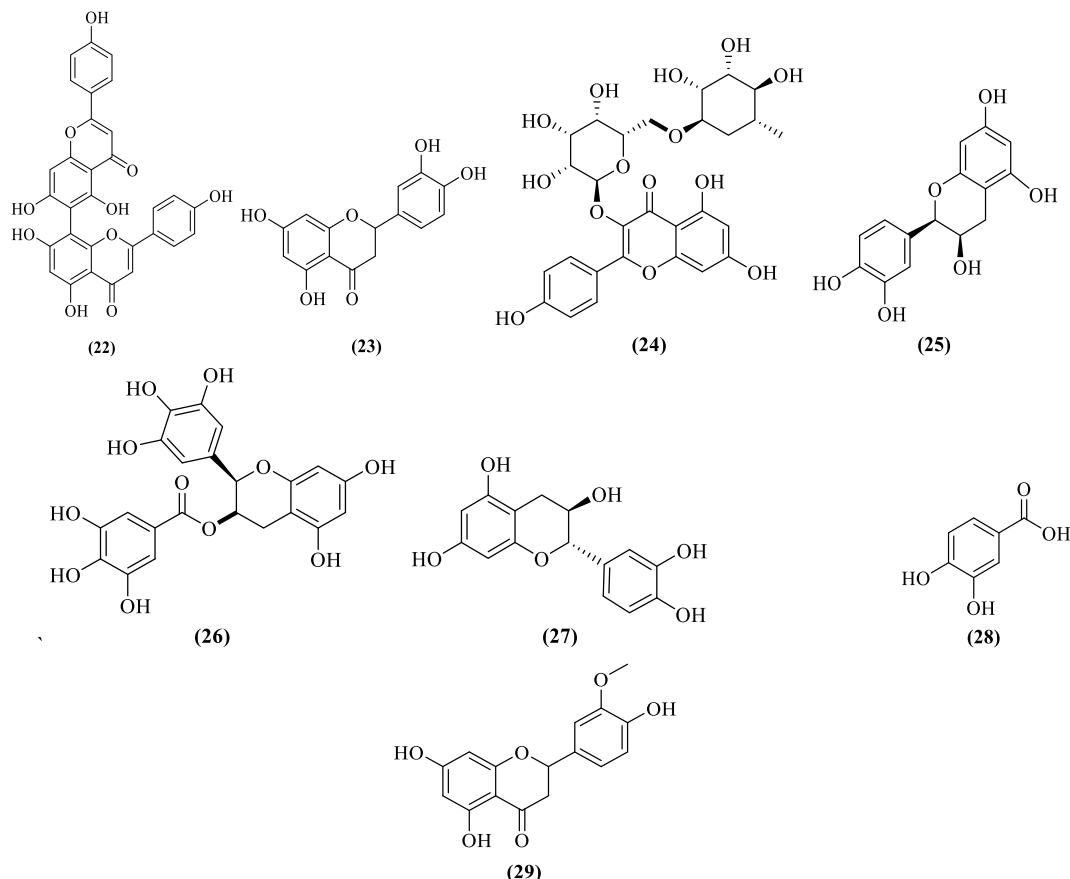


Figure 9. DENV NS2B-NS3 pro inhibitors from natural sources.

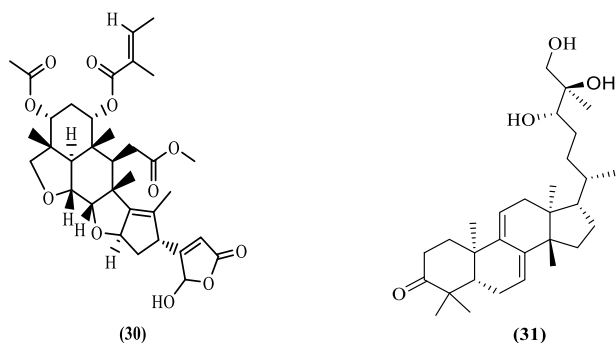


Figure 10. DENV NS2B-NS3 pro inhibitors from natural sources.

of $15.1 \pm 2.2 \mu\text{M}$ and $17.5 \pm 1.4 \mu\text{M}$ against DENV2 and DENV3 pro, respectively. Molecular docking studies with DENV3 pro (PDB 3U11) predicted and identified an allosteric binding site, putative for other non-competitive inhibitors.⁶⁷ Further, Ispita et al. (2019) performed in-silico screening and pharmacokinetic evaluation of 10 established phytoconstituents of *Carica papaya*. Molecular docking studies using the X-ray crystal structure of DENV2 pro (2FOM) identified two flavonoids, apigenin, and luteolin, with the best docking score (-7.7 kcal/mol). However, luteolin (**23**, Figure 9) was considered a more preferred lead owing to its predicted interaction with the residues of the catalytic triad. Luteolin was also predicted to be involved with two identified key residues (Asp75 and Gly153) via hydrophobic interactions.⁶⁸ Recently, Dwivedi et al. studied the anti-DENV properties of *Azadirachta indica*. Virtual screening exercise on 49 reported bioflavonoids against DENV pro helped identify four potential DENV NS2B-NS3 pro inhibitors viz kaempferol-3-O-rutinoside (-9.55 kcal/mol), rutin (-9.32 kcal/mol), hyperoside (-7.87 kcal/mol), and epicatechin (-7.62 kcal/mol). The interaction responsible for the predicted high docking score of kaempferol-3-O-rutinoside (**24**, Figure 9) were six hydrogen bonds between NS3 protease-kaempferol-3-O-rutinoside complex, involving key residues Asp75, Gly151, and Asn152, and other critical residues involved in hydrophobic interactions were His51, Lys73, Pro132, Ser135, Val154, and Tyr161. In addition, residues Gly151 and Gly153 also contributed toward glycine interactions. Cell viability and the in-vitro antiviral studies done on reference compound quercetin, kaempferol-3-O-rutinoside, and epicatechin (**25**, Figure 9) showed kaempferol-3-O-rutinoside as a potent DENV inhibitor (77.7% at 100 μM) and epicatechin (66.2% at 1000 μM) as a moderate inhibitor when compared to quercetin.⁶⁹ In recent work, Farooq et al. (2020) adopted the molecular docking approach with the additional incorporation of antimicrobial and antioxidant activity and identified nine bioactive compounds from *Carica papaya*, of which three compounds viz. epigallocatechin (**26**, Figure 9), catechin (**27**, Figure 9), and protocatechuic acid (PCA, **28**, Figure 9) showed good binding affinities with DENV NS2B-NS3 pro in the in-silico studies. These three compounds were predicted to show strong interaction with the residues of the catalytic triad (His51, Asp75, and Ser135) of DENV pro.⁷⁰

In 2019, Lim et al. isolated six compounds from *Ganoderma lucidum*

Var. *antler*. Molecular docking studies revealed, Hesperitin, a bioflavonone (**29**, Figure 9), as a DENV2 pro inhibitor among the six identified compounds. Also, docking affinities of hesperitin were near the reference ligand, 4-hydroxypanduratin A. Further HOMO-LUMO calculations also indicated good ligand-protease interaction. Hesperitin appeared to interact with the residues of the catalytic triad (His51, Asp75, and Ser135) and oxyanion hole through hydrogen bonding, van der Waal, and hydrophobic interactions.⁷¹

6.2.2.2. Terpenoids. Dwivedi et al. (2016) explored the in-silico inhibitory potential of five triterpenoids obtained from neem plant against DENV NS2B-NS3 pro. Using the crystal structure of DENV NS2B-NS3 pro (PDB 2VBC) for molecular docking, they reported the binding affinities of three triterpenoids viz. Nimbin, desacetylnimbin, and desacetylsalannin to be 5.56, -5.24, and -3.43 kcal/mol, respectively. The high binding affinity of Nimbin (**30**, Figure 10) was attributed to four predicted hydrogen bonds of Nimbin with the enzyme, which included three bonds with the residues of the catalytic triad (His51, Asp75, Ser135) and one with Asn152 residue. In addition, a hydrophobic interaction with six other residues, including the key residues Val154, Pro132, and Gly153, also contributed toward binding affinity.⁷² Bhargava et al. (2019) explored *Ganoderma lucidum* for anti-DENV infection treatment. Before this, *G. lucidum* was reported to have a pool of bioactive compounds, including polysaccharides and triterpenes.⁷³ Several medicinal properties were attributed to *G. lucidum*, including antiviral activity against HIV.⁷⁴ Structure-based virtual screening of 22 triterpenoids, known for their antiviral activities against crystal structure DENV2 pro (PDB 2FOM), identified four triterpenoids with a docking score higher than the reference inhibitor. The triterpenoid Ganodermanontriol (**31**, Figure 10), with a docking score of -6.291 kcal/mol, showed three hydrogen bonding interactions, including key residues Lys73 and Asn167. Besides this, residues involved in hydrophobic interactions included Val154 and Val155. Residues His51, Asn152, and Asn167 were predicted to be involved in polar interaction, while Gly153 was involved in glycine interaction. In addition, positive charge interaction with Lys73 and Lys74, and negative charge interaction with Asp75 residues also contributed to the effective binding. The in-vitro DENV inhibition assay of this compound showed a 40% reduction in viral titer at 50 μM concentration.⁷⁵

6.2.2.3. Curcumin and its analogs. In a previous HTS study, Balasubramanian et al. identified curcumin (unpublished report) as a DENV NS2B-NS3 pro inhibitor.⁷⁶ However, poor plasma availability of curcumin, owing to *retro*-aldol conversion to ferulic acid at the plasma pH^{77,78} prompted them to synthesize four analogs. Although DENV pro inhibitory assays showed modest activity for the analogs (IC_{50} between 36.23 and 60.98 μM), inhibition of DENV replication in the replicon-based assay was promising. A cyclohexanone analog (**32**, Figure 11) of curcumin showed an EC_{50} value of $8.07 \pm 1.52 \mu\text{M}$, whereas EC_{50} for plaque assay was $2.34 \pm 0.21 \mu\text{M}$. Compared to curcumin, a cyclopentanone (**33**, Figure 11) analog with a selectivity index (SI) of 16.27 was the most active and less toxic.⁷⁹ In another effort to synthesize curcumin analog, Zamri et al. (2019) reported a benzenesulphonyl curcumin analog (**34**,

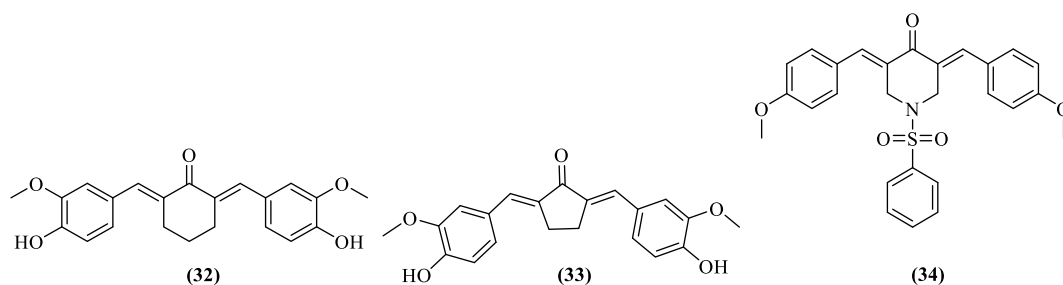


Figure 11. DENV NS2B-NS3 pro inhibitors from natural sources.

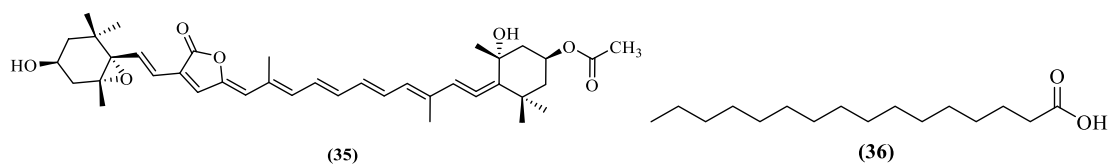


Figure 12. DENV NS2B-NS3 pro inhibitors from natural sources.

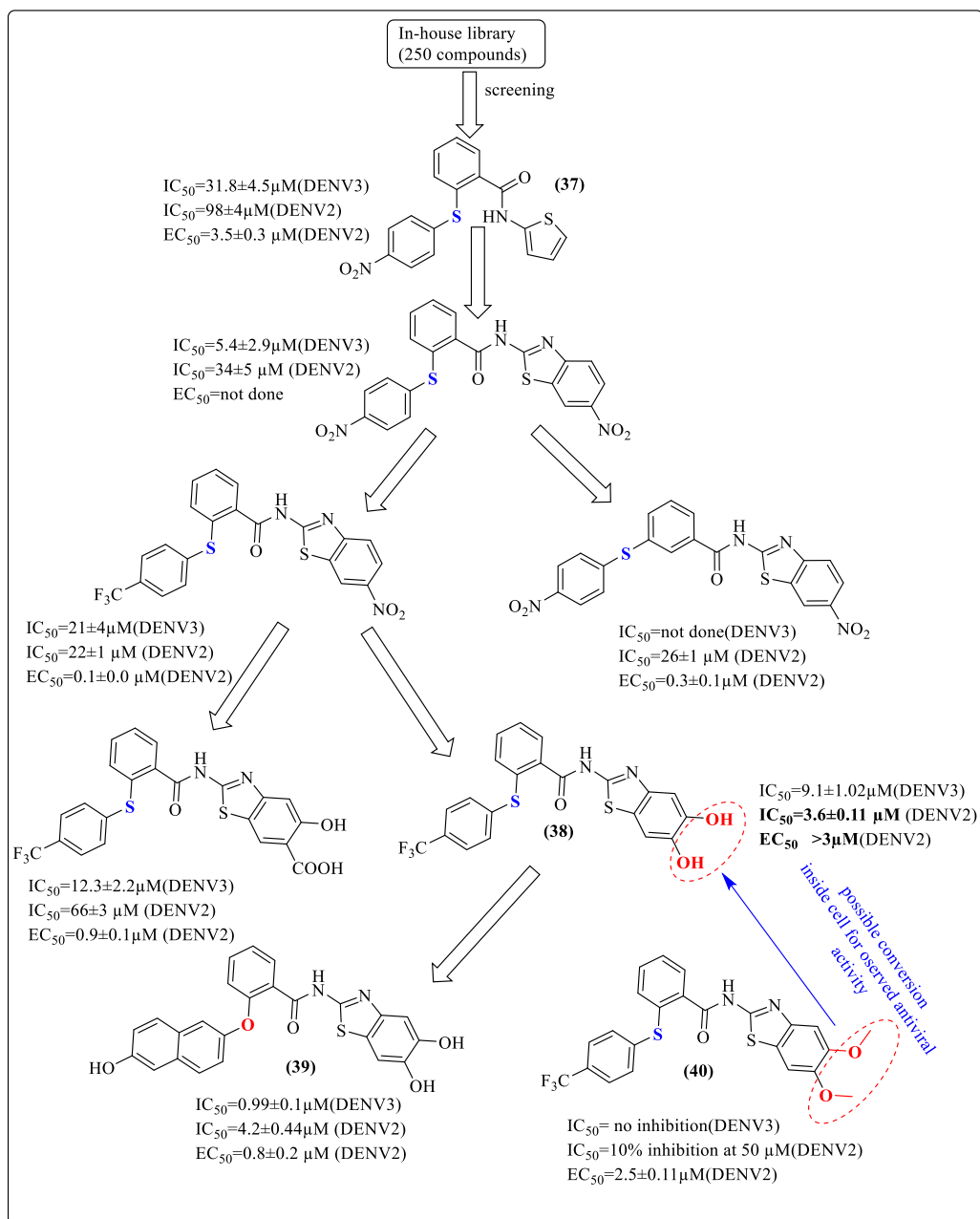


Figure 13. Schematic representation of Wu et al. (2015) modification of lead obtained through HTS.

Figure 11), ((3E,5E)-3,5-bis(4-methoxybenzylidene)-1-(phenylsulfonyl)piperidin-4-one), and in-silico studies revealed promising DENV NS2B-NS3 pro inhibitory activity attributed to the predicted interactions with His51, Asp75, and Ser135 of the catalytic triad. MD simulations showed binding free energy of -61.01 kcal/mol when compared to -59.78 Kcal/mol of the positive control, Panduratin A.⁸⁰

6.2.2.4. Miscellaneous. To identify anti-dengue agents from natural

products, Lee et al. (2016) reported the anti-dengue activity of peridinin (35, Figure 12), a carotene-like substance, for the first time. Peridinin, along with eight other compounds, was obtained from the ethanolic extract of Formosan zoanthid, *Palythoa mutuki*. Their in-vitro potential for inhibiting DENV2 replication was assessed. Peridinin inhibited DENV2 in-vitro replication with an EC_{50} of 4.5 ± 0.46 μM , while EC_{50} reported for the other three serotypes ranged between 5.84 and 7.62 μM . Further, Peridinin proved to be an effective DENV2 pro inhibitor with an

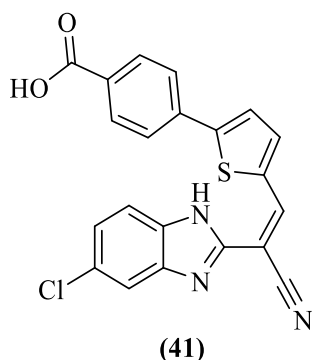


Figure 14. DENV NS2B-NS3 pro inhibitors obtained from HTS.

EC_{50} of $8.5 \pm 0.41 \mu\text{M}$.⁸¹ Tataringa et al. made the first attempt to perform an in-silico study of 11 compounds from the GC-MS analyzed, Romanian *Allium cepa* oil. All the 11 compounds were docked to the seven selected protein targets of DENV, including DENV NS2B-NS3 pro. Hexadecanoic acid (**36**, **Figure 112**) emerged as the best compound with the best binding affinity against almost all the protein targets, including the protease target. It was predicted to form two hydrogen bonds with the protease target.⁸²

However, flavonoids are known to yield false-positive activities in biochemical assays. We observed that none of the original studies have discussed assay interference properties of compounds obtained from natural sources. Upon analyzing all the compounds among those compounds obtained from natural resources, we found that seven out of total of 15 compounds were found to have PAINS groups. Of these, four compounds had catechol moiety while three others had ene-one-ene configuration. Considering these findings, we believe that although promising, the data obtained after studying natural compounds, especially those from the flavonoid class cannot be relied upon completely due to false findings.

6.2.3. Inhibitors from HTS

6.2.3.1. Benzothiazole and benzimidazole derivatives. HTS remains an effective tool for screening compounds to identify lead compounds from a library of the molecules. Wu et al. (2015), to identify new chemical scaffolds for inhibition of the DENV2-3 pro, performed HTS using an in-house library of approximately

250 compounds and identified a lead molecule containing diarylthioether (**37**, **Figure 13**). Modifications to improve the affinity resulted in the synthesis of seven analogs. Significant modifications included thiophene ring replacement with alkyl chain and other heteroaromatic ring systems. Further modifications saw the amide bond replacement with ester and amino groups. However, substitution with alkyl chain, ester, and amine groups led to the loss of activity. As shown in **Figure 13**, subsequent replacements led to the identification of compound **38** (**Figure 13**), which gave the best IC_{50} ($3.6 \pm 0.11 \mu\text{M}$) against DENV2 pro and with a non-competitive mode of inhibition. Docking studies of compound **38** predicted the interaction of one -OH group with the side chain of Asn152 and with the backbone of Lys74 while that of the second -OH group with Lys73. However, a dimethoxy substitution, compound **40** (**Figure 13**), was found to be inactive. Further replacement of CF_3 -Ph by OH-Naphthyl group and "S" by "O" yielded compound **39** (**Figure 13**), which had an IC_{50} of $4.2 \pm 0.44 \mu\text{M}$ against DENV2 pro. Results of the viral replication assay showed low EC_{50} values for most compounds. A remarkable finding was that the dimethoxy derivative, compound **40**, showed a good reduction in viral titer against DENV2, with an EC_{50} value of $2.5 \pm 0.11 \mu\text{M}$. However, it was inactive in the protease assay. In contrast, the findings for compound **38** were the opposite. Compound **38** was not active at a concentration below $3 \mu\text{M}$ in the antiviral assay. Further, it was hypothesized that compound **40** was a prodrug, which gets demethylated to the dihydroxy form to exhibit the action.⁸³

In yet another work, Raut et al. (2015) randomly screened ~ 1000 small molecules from an 'in-house' library to identify potential dengue protease inhibitors. A benzimidazole derivative, compound **41** (**Figure 14**), emerged as the most potent inhibitor of DENV2 pro (IC_{50} =

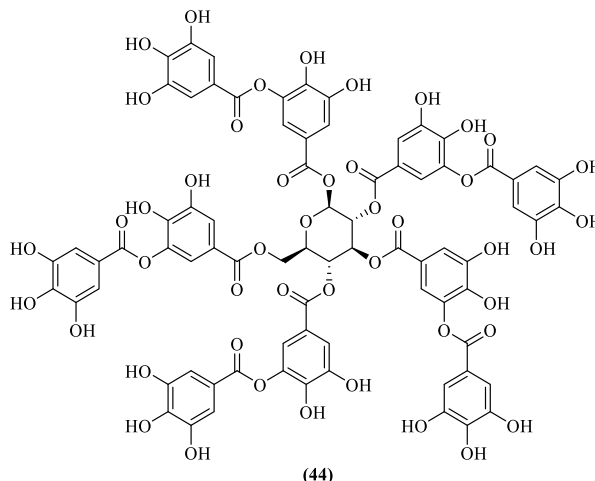
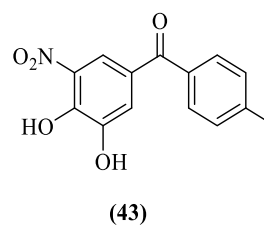
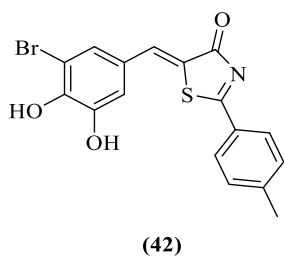


Figure 15. DENV NS2B-NS3 pro inhibitors obtained from HTS.

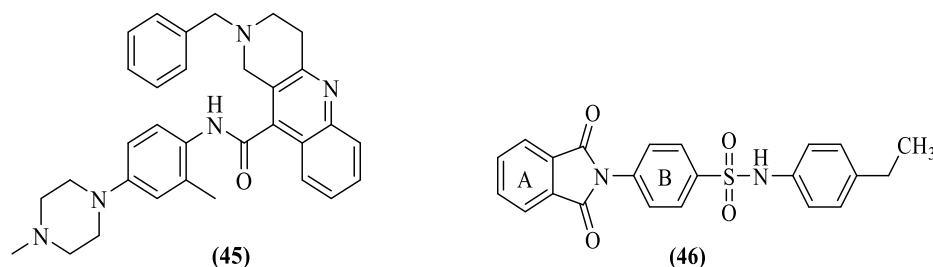


Figure 16. DENV pro inhibitors obtained from HTVS.

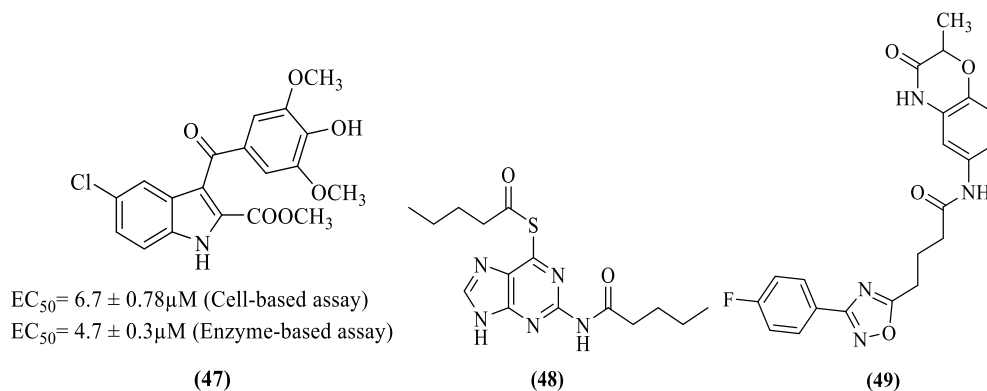


Figure 17. DENV pro inhibitors obtained from HTVS.

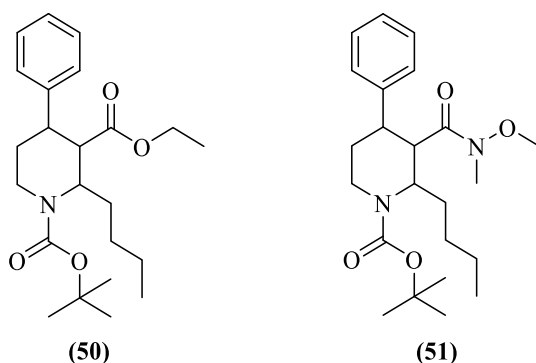


Figure 18. Potent inhibitors of Gan et al. (2017).

5.95 μM). Enzyme kinetic studies indicated a mixed-type inhibition; this was effective against all other DENV serotypes and reduced the viral titer of DENV-1, 2, 3, 4 by 50, 83, 75, and 73% respectively in a cell-based inhibition assay. Docking analysis predicted inhibitor binding to an allosteric site near the active site.⁸⁴

6.2.3.2. Polyphenolic and catechol scaffolds. Balasubramanian et al. (2016) also employed the HTS approach to screen approximately 1,20,000 compounds against DENV2 pro and identified compounds with polyphenolic and catechol scaffolds. Of the eight thoroughly investigated compounds, three compounds (42, 43, and 44, Figure 15) were potent inhibitors of all four serotypes. Their DENV 1–4 pro inhibitory concentrations (IC_{50}) were found to be in the range of 2.94–4.06 μM , 0.64–1.15 μM , and 0.13–0.77 μM , respectively, while the EC_{50} values obtained from DENV2 replication inhibition assay using BHK21 cells for compounds 42 and 43 were $6.9 \pm 0.6 \mu\text{M}$ and $2.29 \pm 0.3 \mu\text{M}$, respectively. All three compounds were competitive inhibitors of DENV2 pro, and molecular docking studies proposed active site binding of all the three inhibitors.⁷⁶

6.2.4. Inhibitors identified through HTVS

HTVS has become an essential part of drug discovery efforts, saving time and providing an opportunity for screening molecules rationally. HTVS, over the years, has helped researchers identify potential HITs and, eventually, potential lead compounds. In the last decade, many antivirals have emerged as a result of this *in-silico* approach.

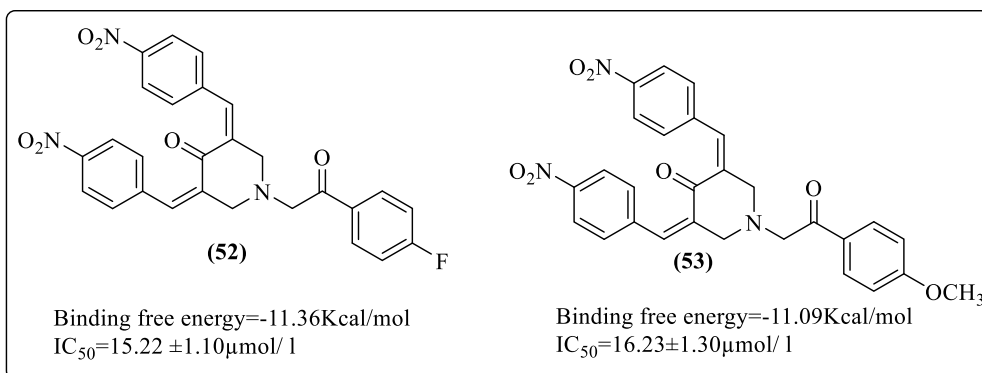


Figure 19. Best reported inhibitors of Osman et al. (2017).

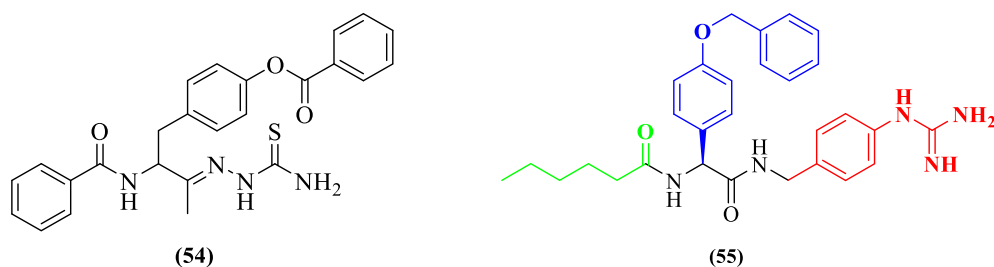


Figure 20. Potent inhibitors of Padampriya et al. (54) and Kühl et al. (55).

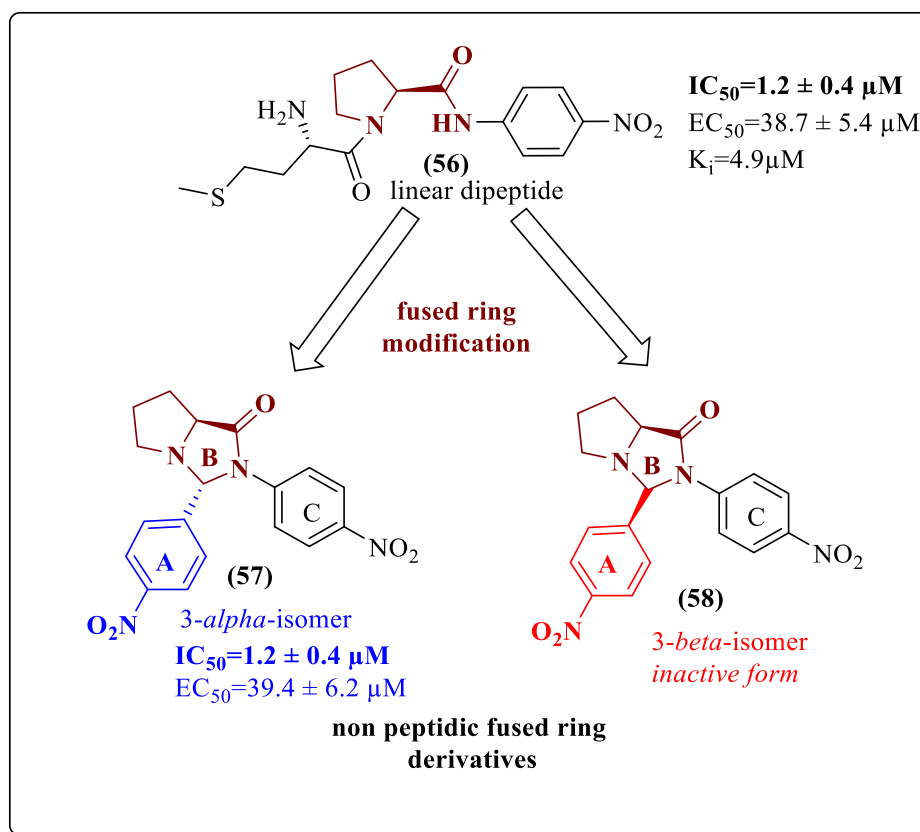


Figure 21. Weng et al. (2017) modification.

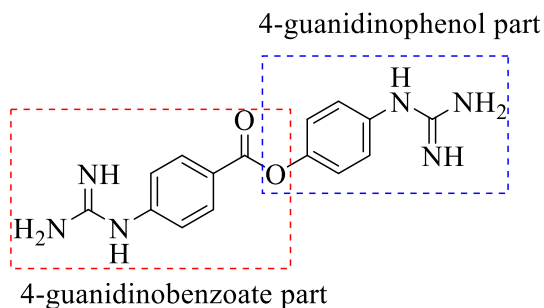


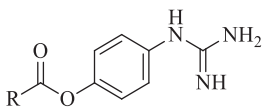
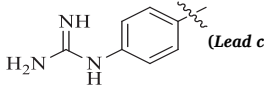
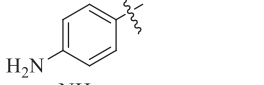
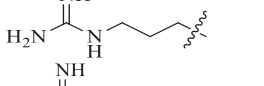
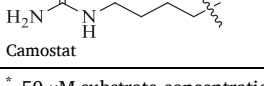
Figure 22. (Lead compound).

6.2.4.1. Piperazine-naphthyridine derivative and isoindoline dione derivatives. Li et al. (2015), through their virtual screening campaign using a library of 5 million compounds obtained from four different commercial sources, attempted structure-guided discovery of a small non-peptide as an inhibitor of DENV2 pro. Fourteen compounds based on docking scores were identified and subjected to biological screening. The top HIT

compound **45** (Figure 16) showed an EC_{50} of $5.0 \mu M$ in BHK21 cells in the protease inhibition assay. Docking study of compound **45** further supported their pharmacophore-based design concept, with a binding free energy of -10.65 kcal/mol . The result was in agreement with the interactions seen in the known crystal structure (PDB 3U11). Also, compound **45** was predicted to occupy the pockets of the binding site, and the benzyl ring of the compound appeared to occupy the hydrophobic region between Pro132 and Val155. Further lone pair of "N" on the adjacent atom was predicted to interact with the hydroxyl group of Tyr161, and an additional π - π interaction could also be seen also it appeared that an additional water molecule linked the amino group of the inhibitor with Met184 and Gly153 to provide stabilization to the inhibitor **45**-protease complex.⁸⁵

Timiri et al. (2015) performed HTVS using the ZINC 8 database against 2FOM to identify an inhibitor of DENV2 pro. After analyzing the top hundred molecules manually, they synthesized phthalimide-sulphonamide derivatives. Twenty derivatives of 4-(1, 3-dioxo-2, 3-dihydro-1H-isoindol-2-yl) benzene- 1-sulphonamide were synthesized and screened for DENV2 pro inhibitory activity. Compound **46** (Figure 16) inhibited protease with an IC_{50} value of $48.2 \mu M$. The

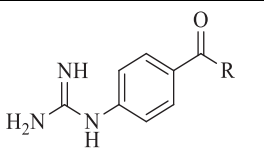
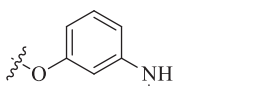
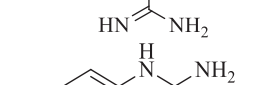
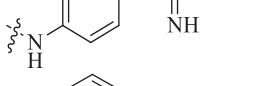
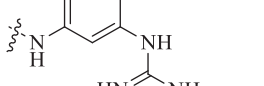
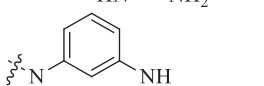
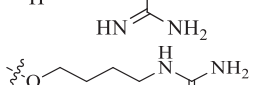
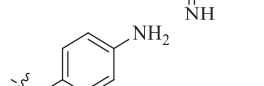
Table 5
Modification of 4-guanidinobenzoate part by Sunderman et al. (2019).

 R	Percentage inhibition of NS2B-NS3 pro	
	DENV ¹	WNV [#]
 (Lead compound)	98.1	29.8
	45.4	No inhibition
	4.2	No inhibition
	4.6	No inhibition
Camostat	19.6	12.6

* 50 μ M substrate concentration and 50 μ M compound concentration.

50 μ M substrate concentration and 25 μ M compound concentration.

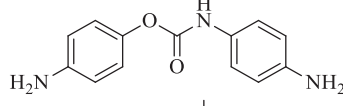
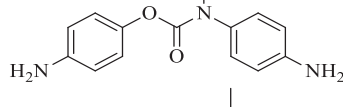
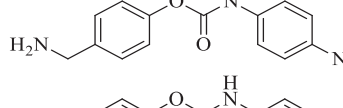
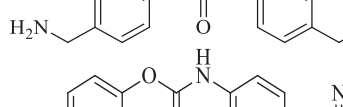
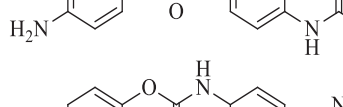
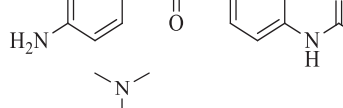
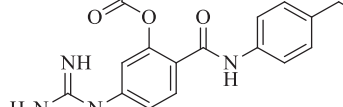
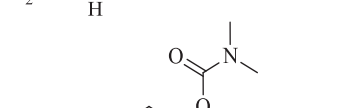
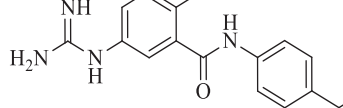
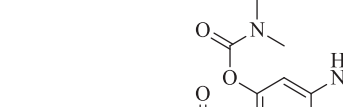
Table 6
Modification of 4-guanidinophenol part by Sunderman et al. (2019).

 R	Percentage inhibition of NS2B-NS3 pro	
	DENV [*]	WNV [#]
	51.3	17.5
	23.2	17.9
	36.8	No inhibition
	56.8	No inhibition
	49.0	17.1
	8.8	No inhibition
	40.1	36.5

* 50 μ M substrate concentration and 50 μ M compound concentration.

50 μ M substrate concentration and 25 μ M compound concentration.

Table 7
Carbamate analogs and their modification by Sunderman et al. (2019).

Compound	Percentage inhibition of NS2B-NS3 pro	
	DENV [*]	WNV [#]
	33.7	72.8
	29.8	68.0
	22.9	59.3
	31.3	62.9
	52.0	61.9
	60.8	68.8
	74.4	73.3
	56.0	76.1
	20.2	23.9
		

* 50 μ M substrate concentration and 50 μ M compound concentration.

50 μ M substrate concentration and 25 μ M compound concentration.

docking score of this compound was -5.12 kcal/mol, and the predicted critical interactions shown by this compound were π - π stacking interactions between ring A and Tyr200, A hydrogen bonding interaction between "O" atom of ring A and "N" atom of imidazole ring in Hip 90. Another hydrogen bonding interaction was observed between the "N" atom attached to sulphonamide and the "O" atom of the carbonyl group of Asn191. They also observed hydrophobic interactions of ring A with Asp168, Phe169, Pro171, Tyr189, Gly190 residues, hydrophobic interaction between 4-ethyl phenyl group attached to sulphonamide and Trp89 and Val111, and a π -cation interaction between electron cloud of ring B and cationic "N" of imidazole ring in Hip90. MD simulations

Table 8
Result of antiviral activity of previously reported inhibitors, Chu et al. (2015).

Sl. No.	Structure	Supplied by	% purity	Ki/EC ₅₀ /IC ₅₀ (Reported)	Cellular toxicity	Antiviral activity	Reason for no antiviral activity	Permeability (P) (10 ⁻⁶ cmS ⁻¹)
1	Ac-RTSKKR-CONH ₂	GL Biochem (China)	>95%	Ki = 12.14 μM	X	X	Inability to permeate & disadvantage of Peptide nature of the drug	0 Not detectible
2		Maybridge (UK)	>95%	Ki = 44 ± 5 μM	X	X	Positive charge on guanidine and basic moiety limitations	0 Not detectible
3	BZ-Ala-Lys-Arg-Arg-H	Mimotopes (Australia)	62%	Ki = 5.3 μM	X	X	Very high charge On compound	0 Not detectible
4		Otava (Ukraine)	>95%	Ki = 17.0 ± 4.3 μM IC ₅₀ = 67.0 ± 7 μM	X	X	High IC ₅₀ value	4.12 ± 0.45
5		Sigma-Aldrich (USA)	>95%	EC ₅₀ = 4.2 ± 1.9 μM	X		Highly permeable	4.45 ± 0.6
6	ARDP0006 	In-house	>95%	Ki = 2.0 μM	X	X	Poor permeability owing to high polarity	0 Not detectible
7		Cambridge Screening Library (USA)	>95%	NR	X	X	Lacked membrane permeability	0 Not detectible
8		Maybridge (UK)	>95%	Ki = 35.7 μM	X	X	Unknown reason	8.40 ± 0.15
9		Cambridge Screening Library (USA)	>95%	Ki = 15 ± 3 μM	X	X	Lacked membrane permeability	0 Not detectible
10		Cambridge Screening Library (USA)	>95%	IC ₅₀ = 27.0 ± 1.3 μM	X	X	Positively charged nature of compound	0 Not detectible
11		GL Biochem (China)	>95%	Ki = 15.6 ± 1.1 μM	X	X	Highly cationic nature of compound	0 Not detectible
12	CGKRKSC 	GL Biochem (China)	>95%	Ki = 1.4 ± 0.1 μM	X	X	Highly cationic nature of compound	0 Not detectible
13	Alexidine hydrochloride	Sigma-Aldrich (USA)	>95%	Ki = 41 ± 3 μM	X	X	Cationic guanidine moieties	0 Not detectible
14	Ivermectin	Sigma-Aldrich (USA)	>95%	Ki = 79 ± 21 μM	—	—	—	—
15	Selamectin	Sigma-Aldrich (USA)	>95%	Ki = 63 ± 18 μM	—	—	—	—

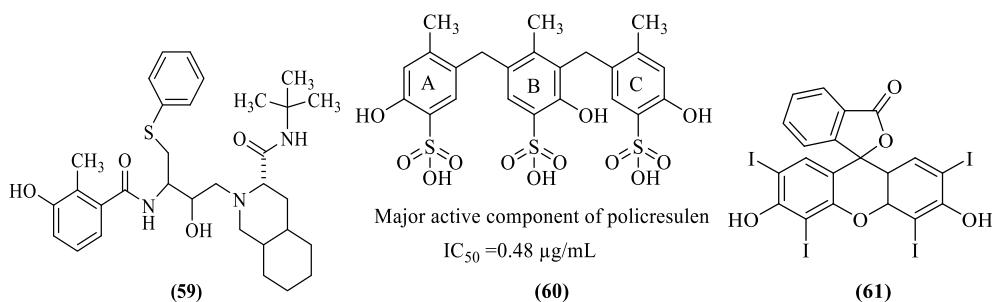


Figure 23. DENV NS2B-NS3 pro inhibitors identified using the drug repurposing approach.

revealed that NS2B-NS3 pro was more stable when bound with inhibitor (46).⁸⁶

6.2.4.2. Indole, Thioguanine and oxadiazole-Aryloxazinone derivatives. Further, Pelliccia et al. (2017) adopted a virtual screening approach to identify allosteric inhibitors against DENV NS2B-NS3 pro. Based on their

findings, they designed and synthesized inhibitors and evaluated their inhibitory potential by performing the cell-based and enzyme-based assay against DENV NS2B-NS3 pro. Among the synthesized compounds, the EC₅₀ values of compound 47 (Figure 17) in the cell-based and enzyme-based assay was found to be 6.7 ± 0.78 μM and 4.7 ± 0.3 μM, respectively. Further, 47 inhibited DENV replication in Huh-7

Table 9
Summary of Patents related to Dengue Protease Inhibitors.

Title	Inventors	Patent number	Related publication (if any)
Small molecule inhibitors of DENV proteases	Viswanathan Usha, Watowich Stanley J	US2015141521A1 US9408813B2	Viswanathan et al. 2014 ¹¹²
Small molecule inhibitors of dengue and WNV proteases	Gilbertson Scott,	US2013035284A1	Tomlinson et al. 2009 ²⁵
Dengue protease substrates and inhibitors	Tomlinson Suzanne M, Watowich Stanley J Harris Jennifer,	US8778876B2 WO2006014232A2	Li et al. 2005 ³¹
Flavivirus protease inhibitors	Li Jun, Tumanut Christine Manzano Mark,	WO2006014232A3 WO2014066502A2	Balsubramanian et al. 2016 ⁷⁶
Dengue and WNV protease inhibitors	Padmanabhan Radhakrishnan, TeramotoTadahisa Harisha Attimogae Shivamurthy,	WO2014066502A3 WO2014164667A1	Kálai et al. 2011 ⁹³
Use of the acetic acid compound 2-[1-[[1-(1-[3-[2-(7-chloroquinolin-2-yl) etenyl] phenyl]-3-[2-(2-hydroxypropan-2-yl) phenyl] propyl] sulfanylmethyl] cyclopropyl] as allosteric inhibitor of the DENV NS2B/NS3 protease	Aldo Segura Cabrera, Carlos Armando García Pérez, Juan Santiago, Salas Benito, Mario Alberto, Rodríguez Pérez	MX2015013285A	NA

cells with an EC₅₀ of 4.60 ± 0.03 μM. Docking studies of this compound predicted the hydrogen bond between the carbonyl portion of the ester and the Asp152 side chain. Also, the ester moiety appeared to be positioned inside the binding pocket. Further, hydrogen bond was predicted between indole, NH and residue Asn167. Residues Val146, Leu149, and Leu76 were predicted to form hydrophobic interaction with the indole ring, and the methoxyphenyl moiety also showed hydrophobic interactions with Trp83 and a π-cation interaction with Lys74.⁸⁷

Hariono et al. (2019) identified a HIT against DENV2 pro by virtual screening a library from the National Cancer Institute database. The experimental IC₅₀ of this HIT was found to be 62 μM against DENV2 pro. Modification of this HIT (having thioguanine scaffold) resulted in a more potent compound (**48**, Figure 17), having an IC₅₀ value of 0.38 μM. Further, from the molecular modeling studies, residues Ser135, Tyr161, and Gly153 were predicted to form hydrogen bonding interactions with the inhibitor (**48**). Few other residues, i.e., Pro132, Gly151, His51, Asp75, and Asn152, appeared to have hydrophobic interactions.⁸⁸ Recently, Bhowmick et al. (2020) performed a multi-step virtual screening of the Asinex database (containing 590,859 compounds) against DENV2 pro using crystal structure 2FOM. The best molecule identified (**49**, Figure 17) had a docking score of -7.619 kcal/mol, and the binding free energy of this molecule calculated from MD simulation trajectories, using the MM/GBSA approach was found to be -60.666 kcal/mol. These metrics were superior to the standard inhibitor (MB21). Further, residues Lys73, Gly153, and Asn167 were predicted to form four hydrogen bonds with the inhibitor (**49**). Residues Lys74 and Leu76 were involved in hydrophobic interactions with the inhibitor, and the only π-cation interaction observed was between Lys74 and inhibitor.⁸⁹

6.3. Inhibitors identified through a rational approach

6.3.1. Piperidinyl and piperidone derivatives

Inspired by their previous studies on natural products and their role as antiviral agents against DENV2, Gan et al. (2017) reported two piperidinyl compounds (**50** and **51**, Figure 18) showing antiviral activity against DENV2 with an EC₅₀ value of 3.2 and 2.4 μM, respectively. Both the compounds were synthesized from nicotinic acid. After the cell-

based assay, protease inhibition was analyzed. However, they were weaker protease inhibitors, as reflected by their IC₅₀ values of 213.7 μM (**50**) and 257.4 μM (**51**).⁹⁰

The 3,5-bis(arylidene)-4-piperidone derivatives have been previously reported for their antiviral,⁹¹ anticancer,⁹² antioxidant,⁹³ and anticholinesterase⁹⁴ activities. The α, β-unsaturated ketone analogs from *Boesenbergia rotunda* were reported to be potent inhibitors of DENV2 serine pro.⁶⁴ In addition, analogs of 4-hydroxypanduratin were also reported as DENV pro inhibitors.⁹⁵ Osman et al. (2017) attempted to exploit the benefits of α, β-unsaturated ketones. They synthesized ten compounds by incorporating a piperidone ring to the α, β-unsaturated ketone system and evaluated their inhibitory activity against DENV2 pro. They performed in-silico studies and correlated the in-silico and in-vitro results. Docking studies using DENV2 pro (PDB 2FOM) identified two inhibitors (**52** and **53**, Figure 19) with good docking scores. These molecules also showed good in-vitro affinities in agreement with the in-silico binding scores. Nitro derivatives of 3, 5-bis (arylidene)-4-piperidones (**52**, **53**) had IC₅₀ values of 15.22 and 16.23 μmol/L, respectively, as compared to the standard panduratin A, which had an IC₅₀ value of 57.28 μmol/L. In molecular docking studies, both compounds appeared to occupy the active site. Compound **52** was predicted to form five hydrogen bonds with the His51, Pro132, Ser135, Gly153, and Arg54 residues. A π-π stacking interaction was also observed between the phenyl ring and His51. Compound **53** was predicted to form six hydrogen bonds with His51, Pro132, Ser135, Gly153, Arg54, and Trp50 residues.⁹⁶

6.3.2. Thiosemicarbazones and 4-benzyloxyphenylglycine derivatives

Considering the biological properties offered by thiosemicarbazones and reports of their role as antiviral agents, Padampriya et al. (2018) synthesized six thiosemicarbazone-derived phenyl-acetyl derivatives and analyzed their in-vitro antiviral activity against the DENV2 serotype. Compound **54** (Figure 20) showed antiviral activity. Its docking study against DENV2 pro (PDB 2FOM) revealed occupancy at the active site where the inhibitor formed four hydrogen bonds with residues Ser135, Gly151, Pro132, and Asp75.⁹⁷ In recent work, Kühl et al. (2020) reported 55 non-peptidic small molecule derivatives of 4-

Table 10

A summary of key residues identified as having interaction with DENV pro.

Key residues of protease	Corresponding pockets/nearby pockets	Type of predicted interactions	Chemical class of compound showing the predicted interactions and their identification number with reference to the manuscript
His 51	S1, S2	Hydrogen bonding interactions, Hydrophobic interactions, π - π interaction	Flavonoids (24, 26, 27), Phenolic acid (28), Bioflavonone (29), Terpenoids (30, 31), Curcumin analogs (34), Thioguanine derivative (48), Piperidone derivative (52, 53), Benzyloxyphenylglycine derivative (55), Pyrrolidino-imidazolidinone derivative (57).
Ser 135	S1	Hydrogen bonding interactions, Hydrophobic interactions, Polar interaction	Flavonoids (24, 26, 27), Phenolic acid (28), bioflavonone (29), Terpenoids (30), Curcumin analogs (34), Thioguanine derivative (48), Piperidone derivative (52, 53), Thiosemicarbazone derivative (54), Pyrrolidino-imidazolidinone derivative (57).
Gly151	S1	Hydrogen bonding interactions, Hydrophobic interactions, Glycine interaction	Flavonoid (24), Thioguanine derivative (48), Thiosemicarbazone derivative (54).
Tyr150	S1	Hydrophobic interactions	Flavonoids (24), Pyrrolidino-imidazolidinone derivative (57).
Tyr161	S1	Hydrogen bonding interactions, Hydrophobic interactions, π - π interaction	Pyrazole ester derivative (19), Flavonoid (24), Piperazine-naphthyridine derivative (45), Thioguanine derivative (48), Decahydroisoquinoline derivative (59).
Tyr215	S1	π - π interaction	Tripeptide (12).
Asp75	S2	Hydrogen bonding interactions, Hydrophobic interactions, Polar interaction	Tripeptides (3), Flavonoids (23, 24, 26, 27), Phenolic acid (28), Bioflavonone (29), Terpenoids (30,31), Curcumin analogs (34), Thioguanine derivative (48), Thiosemicarbazone derivative (54).
Asn152	S2	Hydrogen bonding interactions, Hydrophobic interactions, Polar interaction	Flavonoids (24), Terpenoids (30, 31), Benzothiazole derivative (38), Thioguanine derivative (48).
Lys74	S2	Hydrophobic interactions, π -cation interaction	Terpenoid (31), Benzothiazole derivative (38), Indole derivative (47), oxadiazole-aryl oxazinone derivative (49).
Lys73	S2	Hydrogen bonding interactions, Hydrophobic interactions	Flavonoids (24), Terpenoids (31), Benzothiazole derivative (38), oxadiazole-aryl oxazinone derivative (49).
Asn167	S2	Hydrogen bonding interactions, Polar interaction	Terpenoids (31), Indole derivative (47), oxadiazole-aryl oxazinone derivative (49).
Met84	S2, S3	Hydrogen bonding interactions	Cyclic peptide (15), Decahydroisoquinoline derivative (59).
Pro 132	S3	Hydrogen bonding interactions, Hydrophobic interactions	Pyrazole ester derivatives (19), Flavonoid (24), Terpenoids (30), piperazine-naphthyridine derivative (45), Thioguanine derivative (48), Piperidone derivative (52, 53), Thiosemicarbazone derivative (54), Pyrrolidino-imidazolidinone derivative (57).
Val155	S3, S4	Hydrophobic interactions, π - σ interaction.	Tripeptide (9), Terpenoid (31), Piperazine-naphthyridine derivative (45).
Gly153	S4	Hydrogen bonding interactions, Hydrophobic interactions, Glycine interaction	Flavonoid (23, 24), Terpenoids (30, 31), Piperazine-naphthyridine derivative (45), Thioguanine derivative (48), Oxadiazole-aryl oxazinone derivative (49), Piperidone derivative (52, 53), Decahydroisoquinoline derivative (59).
Val154	S4	Hydrophobic interactions	Flavonoid (24), Terpenoid (30, 31).

Note: Similar color residues share similar properties by virtue of their side chains.

benzyloxyphenylglycine as DENV2 pro inhibitors. In their work, the core 4-benzyloxyphenylglycine was coupled to a lipophilic alkyl chain via an amide bond. The carboxyl portion was further connected via another amide bond to a phenyl group with further variations in basic residues. Variants were produced by fragment merging using biochemical assays for categorizing and combining most active residues. Compound 55 (Figure 20) (the L-isomer), a phenyl guanidine variant, yielded upper-nanomolar DENV2 pro-HeLa EC₅₀ (0.49 ± 0.08 μM) activity. The D-isomer of 55 was found to have 20-fold low potency compared to L-isomer, partly indicating a different binding mode. An added hexanoic acid cap at N-terminal improved the activity of 55 over other substituents. Modeling studies performed against DENV3 pro (PDB 3U11) revealed that the positively charged phenylguanidine moiety was positioned in the S₁ pocket-forming an ionic interaction with the negatively charged aspartate residue. The S₂ pocket was occupied by (4-Benzyloxy)-L-phenylglycine, and the phenyl ring of the phenylglycine formed π - π -stacking interaction with catalytic histidine. The hexanoic acid contributed to lipophilic interactions and occupied the S₃ pocket.⁹⁸

6.4. Inhibitors reported by modification of previously reported inhibitors

Weng et al. modified their previously reported most potent linear

dipeptide DENV2 pro inhibitor.⁹⁹ They synthesized a series of 16 newly fused bicyclic compounds of pyrrolidino[1,2-c] imidazolidinone derivatives and evaluated their inhibitory activity against DENV2NS2B-NS3 pro and wild-type DENV-2 virus. The C-3 stereochemistry of the fused ring system played a crucial role in determining the activity of the fused ring derivatives. The linear dipeptide (56) and a non-peptidic fused ring derivative (57, Figure 21) showed a similar activity profile. Both had an IC₅₀ value of 1.2 ± 0.4 μM and had almost similar EC₅₀ values of 38.7 ± 5.4 μM and 39.4 ± 6.2 μM, respectively. Also, the 3-beta isomer (58, Figure 21) was inactive; thus, the importance of absolute configuration at this position could be understood. Meanwhile, their CC₅₀ values indicated that they had no cytotoxic effect in the tested concentration range. The 3-alpha isomer of the fused ring scaffold was studied with the help of molecular docking against the chain-A of the X-ray crystal structure of DENV2 pro (PDB 2FOM) to understand the interactions which could be attributed to the protease inhibition activity. It was predicted that ring A (p-Nitro phenyl group) occupied the cleft of Tyr150, Ser135, and Pro132. A hydrogen bond was predicted between the oxygen atom of the nitro group of ring A and Ser135 of the catalytic triad. Further, fused ring B, N-4 nitrogen atom appeared to be involved in hydrogen bond formation with imidazole of His51 by donating its lone pair. Ring C was close to Gly133, Ile36, and Val52. The two

Table 11
Few selected potent molecules from different classes.

Chemical class/molecule	Compound No.	IC ₅₀ / EC ₅₀	Activity (inhibition)
Peptides			
Tripeptide	9	IC ₅₀ = 0.018 μM	DENV2 pro
Cap-Arg-Lys-Phe-NH ₂			
Cyclic peptide	15	IC ₅₀ = 0.95 μM.	DENV2 pro
Small molecules			
Pyrazole ester derivative	20	IC ₅₀ = 0.5 ± 0.1 μM	DENV2 pro
Peridinin	35	EC ₅₀ = 4.5 ± 0.46 μM	DENV2 replication
From HTS	38	IC ₅₀ = 3.6 ± 0.11 μM	DENV2 pro
	43	EC ₅₀ = 2.29 ± 0.3 μM	DENV2 replication
From HTVS	47	EC ₅₀ = 4.60 ± 0.03 μM	DENV2 replication
Rational approach			
Piperidinyl derivative	51	EC ₅₀ = 2.4 μM	Antiviral against DENV2
4-benzyloxyphenylglycine derivatives	55	EC ₅₀ = 0.49 ± 0.08 μM	DENV2 pro HeLa EC ₅₀
Drug repurposing			
Nelfinavir	59	EC ₅₀ = 3.5 ± 0.4 μM	Antiviral against DENV2
Policresulen	60	IC ₅₀ = 0.48 μg/mL	DENV2 pro
Erythrosin B	61	EC ₅₀ = 1.2 μM	Antiviral against DENV2

hydrogen bonds formed with the residues of the catalytic triad thus indicated stable binding of the inhibitor with the protein and eventually inhibiting the catalytic activity of the serine protease. Although the EC₅₀ values were not very promising, this study could provide a new approach for discovering non-peptidic DENV pro inhibitors in the future.¹⁰⁰

In yet another modification effort, Sunderman et al. (2019) modified a previously reported dibasic 4-guanidinobenzoate, which inhibited DENV2 pro in the low micro-molar range.¹⁰¹ Their objective was to study the SAR and improve the drug-likeness of lead compounds (figure 22). Earlier Aryl-4-guanidinobenzoates were known for the formation of reversible or pseudo-irreversible covalent bonds.¹⁰² Also, the replacement of the ester group with amide and the introduction of carbamates between two aromatic rings was associated with inhibition of serine protease activity.¹⁰³ These changes were incorporated in the lead structure, and 19 analogs of the lead were synthesized and evaluated for DENV2 and WNV pro inhibition. These results have been summarized in (Table 5-7). The 4-guanidinobenzoate modifications (Table 5) showed that the activity decreased when the aromatic ring was replaced with the aliphatic chain. The 4-guanidinophenol modifications (Table 6) also did not yield encouraging results. However, they were more effective when compared to the 4-guanidinobenzoate modifications. The introduction of the carbamate group between the aromatic groups also resulted in less active compounds (Table 7) as they showed weak inhibitory activity. SAR studies on these compounds established the importance of the electrophilic ester group and 4-guanidinobenzoate for protease inhibition. Also, it indicated that 4-guanidinophenol modification was more acceptable than 4-guanidinobenzoate modification. Binding mode analysis for the lead compound showed covalent interaction with DENV pro. However, stability in the basic buffer remained a significant concern.¹⁰⁴

These two modifications yielded successful results. Although the results were not highly encouraging, the insights from these studies certainly improve our understanding of the dos and don'ts in the drug design process.

6.5. Inhibitor reported by investigation of antiviral activities of previously reported inhibitors

Chu et al. (2015) investigated the antiviral activities of 15 small molecule and peptide-based NS2B-NS3 pro inhibitors on dengue serotype 2-infected HuH-7 human hepatocarcinoma cells. Experimental results revealed an anthraquinone (ARDP0006) as the most potent inhibitor, which reduced dengue viral titer by >1 log PFU/mL at 1 μM concentration in their cell-based assays involving HuH-7 and K562 cell lines. It was also non-cytotoxic at 1 μM concentration over three days of

incubation on HuH-7 cells using the Alamar Blue cellular toxicity assay. Table 8 summarizes the work done by this group. The key conclusion of their study was that, although a molecule was an effective DENV2 pro inhibitor, the potential to be a successful drug candidate lay in its ability to penetrate the cells chosen for the study and reduce viral titer. Ideally, DENV2 pro inhibitors should be amenable to modifications that enhance the permeability, which is indicated by their PAMPA values. This molecule could be exploited for drug development in the future.¹⁰⁵

6.6. Inhibitors from drug repurposing (Nelfinavir, Policresulen, and Erythrosin B)

Drug refocusing as a concept has gained significant popularity with the emergence of the COVID-19 pandemic. Similar approaches have also been used for DENV drug discovery. Bhakat et al. (2015) first reported drug repurposing efforts where they analyzed nine peptidomimetic FDA-approved HIV/HCV inhibitors by molecular docking and using a cell-based antiviral assay. Docking of the HIV/HCV inhibitors was done using the closed conformation of DENV NS2B-NS3 pro (PDB 3U11), and the results predicted that the HIV/HCV inhibitors were able to bind the active sites of DENV NS2B-NS3 pro. The results were further refined using MD-based MM/GBSA rescoring, and it was observed that van der Waals interactions were the key driving forces for the inhibitor-enzyme interactions in the active site. Nelfinavir (Decahydroisoquinoline scaffold derivative, 59, Figure 23) showed hydrogen bonding interactions with Met84 and Gly153, a π-π stacking interaction with Tyr161, and a side chain hydrogen bond interaction with Thr83 also contributed to the binding.

Interestingly the docking score of Nelfinavir (-8.9 kcal/mol) complimented the antiviral cell-based assay results. Nelfinavir showed the best antiviral activity against DENV-2 with EC₅₀ of 3.5 ± 0.4 μM and a SI of 4.6.¹⁰⁶ Further, Wu et al. (2015), from their in-house library of old drugs (~1000 compounds), identified a topical hemostatic and anti-septic 2-hydroxy-3,5-bis [(4-hydroxy-2-methyl-5-sulphophenyl) methyl]-4-methyl-benzene-sulfonic acid (Policresulen) as a potent inhibitor of DENV2 pro with an IC₅₀ value of 0.48 μg/mL. Policresulen acted as a competitive inhibitor of the protease and slightly affected protease stability. Also, policresulen inhibited DENV2 replication in BHK-21 cells giving an IC₅₀ value of 4.99 μg/mL. Furthermore, IC₅₀ for cytotoxicity to BHK-21 cells was found to be 459.45 μg/mL. Policresulen is a mixture of various analogs.¹⁰⁷ Compound 60 (Figure 23) represents the major component of policresulen, and for a better understanding of the binding interaction, it was docked with the structural NS2B-NS3 pro model (PDB 2M9Q). The study predicted that in ring A, sulfo group oxygen appeared to form a hydrogen bond with the Gln106 side chain in the P1 region of the protease. The phenol group formed hydrogen bonds with the main

chain carbonyl of Gln114. Ring B formed hydrophobic interactions with Ile109, Ile115, and Val 131 in the hydrophobic P2 region of the protease. An electrostatic interaction was also seen between the sulfo group and His130. In the ring C, the oxygen of the sulfo group formed a hydrogen bond with side chain residues of Thr132 and Arg133 in the positive P3 region of the protease.¹⁰⁸ Recently, Li et al. reported Erythrosin B (EB) (61, Figure 23), an FDA- approved food additive, as a potent inhibitor of flaviviruses, including DENV pro with low IC₅₀ value. They used their previously developed split luciferase complementation (SLC) based HTS assay to identify molecules blocking the interaction between NS2B and NS3 of DENV2 pro.¹⁰⁹ EB non-competitively inhibited the interaction between DENV2 NS2B and NS3 with an IC_{50-SLC} value of 15 μM. The antiviral efficacy of EB was evaluated using viral plaque reduction assay, and EC₅₀ determined against DENV2 was 1.2 μM. Since inhibitors targeting NS2B-NS3 interaction sites are potentially broad-spectrum inhibitors for flaviviruses,^{109,110} EB's potential to inhibit other flaviviruses was also investigated, and results were encouraging. Viral titer reduction was found to be dose-dependent in other flaviviruses.¹¹¹

6.7. Clinical trials and patents

We searched for dengue fever in the clinical trials database (<https://clinicaltrials.gov>) and found only 19 records reflecting drug trials. A summary of the patents available for dengue protease inhibitors is provided in Table 9; none of these records reflected any protease inhibitors.

7. Conclusion

Despite best efforts by various research groups over the years, none of the DENV protease inhibitors has entered clinical trials. The failure of the only vaccine developed has further increased the demand for the search for a potent drug. The structure and function of DENV protease is well understood. Based on the efforts made by researchers in the industry and academia, it is well understood that aiming only to develop inhibitors with sub-micromolar or nanomolar affinities will not serve the purpose. The fundamental challenge in developing an effective drug lies in dealing with the toxicity, stability, and permeability of DENV protease inhibitors. Improving the permeability of the peptide inhibitors while maintaining the protease inhibitory profile requires a balanced selection of functional groups to be incorporated in the design. One such attempt was made by Takagi et al. while designing the cyclic peptides, where they found the introduction of aromatic residues in the design improved the inhibitory profile. Also, in general, the peptide inhibitors showed marked improvement in protease inhibition by aromatization of N & C-terminals. An insight into the protease inhibitor interaction provided by the different research groups in their work lead us to identify certain key residues which could be targeted using a rational design approach. Since these residues of DENV protease appear to be involved in a variety of interactions as shown in Table 10 (hydrogen bonding interactions, hydrophobic interactions, π - π interaction, π -cation interaction, glycine interaction, polar interaction, π - σ interaction) and since the chemical scaffolds with which they interacted belonged to diverse chemical classes, this advantage could be leveraged in drug design approach, both for the designing the small molecule inhibitors as well as peptide inhibitors. Importantly the identified key residues showed interaction with more than half of the reported inhibitors. Table 10 shows the key residues of the proteases which interacted with the inhibitors having a wide range of chemical scaffolds in their architecture. It can be seen that the residues of the catalytic triad and residues Asn152, Pro132, Lys73 were commonly engaged in hydrogen bonding and hydrophobic interactions. In contrast, certain residues like Tyr161 (π - π interaction), His51 (π - π interaction), Gly153 (Glycine interaction), Lys74 (π -cation interaction), Val155 (π - σ interaction) showed some characteristic interactions confined to these residues. Exploring the occupancies of S1, S1, S2, S3, and S4 pockets by different scaffolds

(Table 10) and the residues interacting with these pockets could help us develop novel scaffolds (peptides and small molecules). At the same time, a rational attempt could be made to address the pharmacokinetic issues of the tripeptide inhibitors by proper substitution of basic residues at P1 and P2 position of tripeptide molecule with different heterocyclic/aromatic/cyclic/bicyclic rings, which were predicted to occupy different positions in the S1 and S2 pockets of different reported inhibitors. Table 10 also provides few hydrophobic scaffolds as possible substitutes of the tripeptide cap group, often appearing to occupy the S3 and S4 sub-pockets of the protease. Hence the scaffolds occupying the S3 and S4 sub-pockets could prove to be good substitutes or other possible substitutes of the cap of the tripeptides, and their utility in enhancing the pharmacokinetic properties could be further tested. Each scaffold with its substitution offers a definite property to the molecule, which is finally responsible for the inhibitory activity. Table 10 summarizes scaffolds present in various compounds. Since we are far from obtaining a small molecule inhibitor with a nanomolar affinity, any combination of scaffolds with moderate inhibition could be rationally selected for further development. While assembling active portions from these scaffolds could yield active molecules, their synthetic feasibility should also be considered. Table 11 presents a summary of potent molecules from different sections. DENV and COVID-19 co-infection has raised serious concerns. The emergence of co-infections inspired us to compare substrate-peptide residue preferences and the residues lining the sub-pockets of both the proteases. To the best of our knowledge, this review is the first attempt to compare the similarities and differences between both proteases. Viral propagation in both the families of viruses is dependent on the activity of the proteases involved. Thus, we believe that our insights on similarities in the residue preferences of both the proteases and the analysis on residues lining the sub-pockets of both the proteases could help new researchers strategize their new drug discovery efforts and guide established researchers to steer their research in this direction. This approach should especially spur the development of peptidomimetics which have shown a significantly potent inhibitory activity in the past. However, this topic needs further exploration since the insights on SARS-CoV-2 3CL^{pro} are relatively fresh. Our group is currently making efforts toward screening the reported DENV NS2B-NS3 pro inhibitors and other libraries in the database against SARS-CoV-2 3CL^{pro}, and we have got encouraging results. The results will be published in the followup manuscript.

Declaration of Competing Interest

The authors declare that they have no known competing financial interests or personal relationships that could have appeared to influence the work reported in this paper.

Acknowledgments

The authors would like to thank the funding agency, DST-SERB, Govt. of India, for providing financial support through their project (EMR /2016/005711) dated 7th August 2017 and Birla Institute of Technology, Mesra, Ranchi, India for providing the necessary infra-structural facilities.

References

- Bhatt S, Gething PW, Brady OJ, et al. The global distribution and burden of dengue. *Nature*. 2013;496:504–507. <https://doi.org/10.1038/nature12060>.
- Ashburn PM, Craig CF. Experimental investigations regarding the etiology of dengue fever. 1907. *J Infect Dis*. 2004;189(9):1747-1783; discussion 1744. <http://doi.org/10.1086/383418>.
- Lescar J, Luo D, Xu T, et al. Towards the design of antiviral inhibitors against flaviviruses: The case for the multifunctional NS3 protein from Dengue virus as a target. *Antiviral Res*. 2008;80:94–101. <https://doi.org/10.1016/j.antiviral.2008.07.001>.

- 4 Stevens AJ, Gahan ME, Mahalingam S, Keller PA. The medicinal chemistry of dengue fever. *J Med Chem*. 2009;52:7911–7926. <https://doi.org/10.1021/jm900652e>.
- 5 Nitsche C, Holloway S, Schirmeister T, Klein CD. Biochemistry and medicinal chemistry of the dengue virus protease. *Chem Rev*. 2014;114:11348–11381. <https://doi.org/10.1021/cr500233q>.
- 6 Kautner I, Robinson MJ, Kuhnle U. Dengue virus infection: Epidemiology, pathogenesis, clinical presentation, diagnosis, and prevention. *J Pediatr*. 1997;131(4):516–524. [https://doi.org/10.1016/S0022-3476\(97\)70054-4](https://doi.org/10.1016/S0022-3476(97)70054-4).
- 7 Simmons CP, Farrar JJ, Van Vinh CaN, Wills B. Current concepts: Dengue. *N Engl J Med*. 2012;366:1423–1432. <https://doi.org/10.1056/NEJMr1110265>.
- 8 Simmons CP, Farrar JJ, van Vinh Chau N, Wills B. Barriers to preclinical investigations of anti-dengue immunity and dengue pathogenesis. *Nat Rev Microbiol*. 2012;366:1423–1432. <https://doi.org/10.1056/NEJMr1110265>.
- 9 Kyle JL, Harris E. Global spread and persistence of dengue. *Annu Rev Microbiol*. 2008;62:71–92. <https://doi.org/10.1146/annurev.micro.62.081307.163005>.
- 10 Guzman MG, Alvarez M, Halstead SB. Secondary infection as a risk factor for dengue hemorrhagic fever/dengue shock syndrome: An historical perspective and role of antibody-dependent enhancement of infection. *Arch Virol*. 2013;158:1445–1459. <https://doi.org/10.1007/s00705-013-1645-3>.
- 11 Halstead SB. Neutralization and Antibody-Dependent Enhancement of Dengue Viruses. *Adv Virus Res*. 2003;60:421–467. [https://doi.org/10.1016/S0065-3527\(03\)60011-4](https://doi.org/10.1016/S0065-3527(03)60011-4).
- 12 WHO. Global Strategy for Dengue Prevention and Control.; 2012. doi:entity/denguecontrol/9789241504034/en/index.html.
- 13 Brady OJ, Gething PW, Bhatt S, et al. Refining the Global Spatial Limits of Dengue Virus Transmission by Evidence-Based Consensus. *PLoS Negl Trop Dis*. 2012;6. <https://doi.org/10.1371/journal.pntd.0001760>.
- 14 World Health Organisation. Dengue and severe dengue. WHO Fact Sheet. Accessed January 5, 2021. <https://www.who.int/news-room/fact-sheets/detail/dengue-and-severe-dengue>.
- 15 Guy B, Noriega F, Ochiai RL, et al. A recombinant live attenuated tetravalent vaccine for the prevention of dengue. *Expert Rev Vaccines*. 2017;16:671–683. <https://doi.org/10.1080/14760584.2017.1335201>.
- 16 Timiri AK, Sinha BN, Jayaprakash V. Progress and prospects on DENV protease inhibitors. *Eur J Med Chem*. 2016;117:125–143. <https://doi.org/10.1016/j.ejmech.2016.04.008>.
- 17 Chambers TJ, Hahn CS, Galler R, Rice CM. Flavivirus genome organization, expression, and replication. *Annu Rev Microbiol*. 1990;44:649–688. <https://doi.org/10.1146/annurev.mi.44.100190.003245>.
- 18 Melino S, Paci M. Progress for dengue virus diseases: Towards the NS2B-NS3pro inhibition for a therapeutic-based approach. *FEBS J*. 2007;274:2986–3002. <https://doi.org/10.1111/j.1742-4658.2007.05831.x>.
- 19 Yusof R, Clum S, Wetzel M, Murthy HMK, Padmanabhan R. Purified NS2B/NS3 serine protease of dengue virus type 2 exhibits cofactor NS2B dependence for cleavage of substrates with dibasic amino acids in vitro. *J Biol Chem*. 2000;275:9963–9969. <https://doi.org/10.1074/jbc.275.14.9963>.
- 20 Bazan JF, Fletterick RJ. Detection of a trypsin-like serine protease domain in flaviviruses and pestiviruses. *Virology*. 1989;171:637–639. [https://doi.org/10.1016/0042-6822\(89\)90639-9](https://doi.org/10.1016/0042-6822(89)90639-9).
- 21 Falgout B, Pethel M, Zhang YM, Lai CJ. Both nonstructural proteins NS2B and NS3 are required for the proteolytic processing of dengue virus nonstructural proteins. *J Virol*. 1991;65:2467–2475. <https://doi.org/10.1128/jvi.65.5.2467-2475.1991>.
- 22 Erbel P, Schiering N, D'Arcy A, et al. Structural basis for the activation of flaviviral NS3 proteases from dengue and West Nile virus. *Nat Struct Mol Biol*. 2006;13:372–373. <https://doi.org/10.1038/nsmb1073>.
- 23 Phong WY, Moreland NJ, Lim SP, Wen D, Paradkar PN, Vasudevan SG. Dengue protease activity: The structural integrity and interaction of NS2B with NS3 protease and its potential as a drug target. *Biosci Rep*. 2011;31:399–409. <https://doi.org/10.1042/BSR20100142>.
- 24 Mukhopadhyay S, Kuhn RJ, Rossmann MG. A structural perspective of the Flavivirus life cycle. *Nat Rev Microbiol*. 2005;3:13–22. <https://doi.org/10.1038/nrmicro1067>.
- 25 Tomlinson SM, Malmstrom RD, Russo A, Mueller N, Pang YP, Watowich SJ. Structure-based discovery of dengue virus protease inhibitors. *Antiviral Res*. 2009;82:110–114. <https://doi.org/10.1016/j.antiviral.2009.02.190>.
- 26 Verduyn M, Allou N, Gazielle V, et al. Co-infection of dengue and covid-19: A case report. *PLoS Negl Trop Dis*. 2020;14:1–5. <https://doi.org/10.1371/journal.pntd.0008476>.
- 27 Epelboin L, Blondé R, Nacher M, Combe P, Collet L. COVID-19 and dengue co-infection in a returning traveller. *J Travel Med*. 2021;27:1–2. <https://doi.org/10.1093/JTM/TAAA114>.
- 28 Saddique A, Rana MS, Alam MM, et al. Emergence of co-infection of COVID-19 and dengue: A serious public health threat. *J Infect*. 2020;81:e16–e18. <https://doi.org/10.1016/j.jinf.2020.08.009>.
- 29 Chambers TJ, Weir RC, Grakoui A, et al. Evidence that the N-terminal domain of nonstructural protein NS3 from yellow fever virus is a serine protease responsible for site-specific cleavages in the viral polyprotein. *Proc Natl Acad Sci U S A*. 1990;87:8898–8902. <https://doi.org/10.1073/pnas.87.22.8898>.
- 30 Preugschat F, Yao CW, Strauss JH. In vitro processing of dengue virus type 2 nonstructural proteins NS2A, NS2B, and NS3. *J Virol*. 1990;64:4364–4374. <https://doi.org/10.1128/jvi.64.9.4364-4374.1990>.
- 31 Li J, Lim SP, Beer D, et al. Functional profiling of recombinant NS3 proteases from all four serotypes of dengue virus using tetrapeptide and octapeptide substrate libraries. *J Biol Chem*. 2005;280:28766–28774. <https://doi.org/10.1074/jbc.M500588200>.
- 32 Woo PCY, Lau SKP, Huang Y, Yuen KY. Coronavirus diversity, phylogeny and interspecies jumping. *Exp Biol Med*. 2009;234:1117–1127. <https://doi.org/10.3181/0903-MR-94>.
- 33 Chan JFW, Li KSM, To KKW, Cheng VCC, Chen H, Yuen KY. Is the discovery of the novel human betacoronavirus 2c EMC/2012 (HCoV-EMC) the beginning of another SARS-like pandemic? *J Infect*. 2012;65:477–489. <https://doi.org/10.1016/j.jinf.2012.10.002>.
- 34 Chan JFW, Lau SKP, Woo PCY. The emerging novel Middle East respiratory syndrome coronavirus: The “knowns” and “unknowns”. *J Formos Med Assoc*. 2013;112:372–381. <https://doi.org/10.1016/j.jfma.2013.05.010>.
- 35 Gorbalenya AE, Baker SC, Baric RS, et al. The species Severe acute respiratory syndrome-related coronavirus: classifying 2019-nCoV and naming it SARS-CoV-2. *Nat Microbiol*. 2020;5:536–544. <https://doi.org/10.1038/s41564-020-0695-z>.
- 36 Wu A, Peng Y, Huang B, et al. Genome Composition and Divergence of the Novel Coronavirus (2019-nCoV) Originating in China. *Cell Host Microbe*. 2020;27:325–328. <https://doi.org/10.1016/j.chom.2020.02.001>.
- 37 Pillaiyar T, Manickam M, Namasiyayam V, Hayashi Y, Jung SH. An overview of severe acute respiratory syndrome-coronavirus (SARS-CoV) 3CL protease inhibitors: Peptidomimetics and small molecule chemotherapy. *J Med Chem*. 2016;59:6595–6628. <https://doi.org/10.1021/acs.jmedchem.5b01461>.
- 38 Yang H, Xie W, Xue X, et al. Design of wide-spectrum inhibitors targeting coronavirus main proteases. *PLoS Biol*. 2005;3. <https://doi.org/10.1371/journal.pbio.0030324>.
- 39 Hilgenfeld R. From SARS to MERS: crystallographic studies on coronaviral proteases enable antiviral drug design. *FEBS J*. 2014;281:4085–4096. <https://doi.org/10.1111/febs.12936>.
- 40 Zhang L, Lin D, Sun X, curth U, drosten c, Sauerhering L, Becker S, Rox K and Hilgenfeld R: Crystal structure of SARS-coV-2 main protease provides a basis for design of improved α -ketoamide inhibitors. *Science* (80-). 2020;368:409-412.
- 41 Zhang L, Lin D, Kusov Y, et al. α -Ketoamides as Broad-Spectrum Inhibitors of Coronavirus and Enterovirus Replication: Structure-Based Design, Synthesis, and Activity Assessment. *J Med Chem*. 2020;63:4562–4578. <https://doi.org/10.1021/acs.jmedchem.9b01828>.
- 42 Zhang Z, Li Y, Loh YR, et al. NS2B-NS3 Protease from Zika Virus. Vol 354.; 2016.
- 43 Ullrich S, Nitsche C. The SARS-CoV-2 main protease as drug target. *Bioorganic Med Chem Lett*. 2020;30, 127377. <https://doi.org/10.1016/j.bmcl.2020.127377>.
- 44 Chuck CP, Chong LT, Chen C, Chow HF, Wan DCC, Wong KB. Profiling of substrate specificity of SARS-CoV 3CLpro. *PLoS ONE*. 2010;5:1–7. <https://doi.org/10.1371/journal.pone.0013197>.
- 45 Hegyi A, Ziebuhr J. Conservation of substrate specificities among coronavirus main proteases. *J Gen Virol*. 2002;83:595–599. <https://doi.org/10.1099/0022-1317-83-3-595>.
- 46 Yang H, Yang M, Ding Y, et al. The crystal structures of severe acute respiratory syndrome virus main protease and its complex with an inhibitor. *Proc Natl Acad Sci USA*. 2003;100:13190–13195. <https://doi.org/10.1073/pnas.1835675100>.
- 47 Dai W, Zhang B, Jiang XM, et al. Structure-based design of antiviral drug candidates targeting the SARS-CoV-2 main protease. *Science* (80-). 2020;368:1331–1335. <https://doi.org/10.1126/science.abb4489>.
- 48 Gahlawat A, Kumar N, Kumar R, et al. Structure-Based Virtual Screening to Discover Potential Lead Molecules for the SARS-CoV-2 Main Protease. *J Chem Inf Model*. 2020;60:5781–5793. <https://doi.org/10.1021/acs.jcim.0c00546>.
- 49 Li Q, Kang CB. Progress in developing inhibitors of sars-cov-2 3c-like protease. *Microorganisms*. 2020;8:1–18. <https://doi.org/10.3390/microorganisms8081250>.
- 50 Behnam MAM, Nitsche C, Vechi SM, Klein CD. C-terminal residue optimization and fragment merging: Discovery of a potent peptide-hybrid inhibitor of dengue protease. *ACS Med Chem Lett*. 2014;5:1037–1042. <https://doi.org/10.1021/ml500245v>.
- 51 Nitsche C, Behnam MAM, Steuer C, Klein CD. Retro peptide-hybrids as selective inhibitors of the Dengue virus NS2B-NS3 protease. *Antiviral Res*. 2012;94:72–79. <https://doi.org/10.1016/j.antiviral.2012.02.008>.
- 52 Nitsche C, Schreier VN, Behnam MAM, Kumar A, Bartenschlager R, Klein CD. Thiazolidinone-peptide hybrids as dengue virus protease inhibitors with antiviral activity in cell culture. *J Med Chem*. 2013;56:8389–8403. <https://doi.org/10.1021/jm400828u>.
- 53 Weigel LF, Nitsche C, Graf D, Bartenschlager R, Klein CD. Phenylalanine and Phenylglycine Analogues as Arginine Mimetics in Dengue Protease Inhibitors. *J Med Chem*. 2015;58:7719–7733. <https://doi.org/10.1021/acs.jmedchem.5b00612>.
- 54 Behnam MAM, Graf D, Bartenschlager R, Zlotos DP, Klein CD. Discovery of Nanomolar Dengue and West Nile Virus Protease Inhibitors Containing a 4-Benzoyloxyphenylglycine Residue. *J Med Chem*. 2015;58:9354–9370. <https://doi.org/10.1021/acs.jmedchem.5b01441>.
- 55 Bastos Lima A, Behnam MAM, El Sherif Y, Nitsche C, Vechi SM, Klein CD. Dual inhibitors of the dengue and West Nile virus NS2B-NS3 proteases: Synthesis, biological evaluation and docking studies of novel peptide-hybrids. *Bioorganic Med Chem*. 2015;23:5748–5755. <https://doi.org/10.1016/j.bmc.2015.07.012>.
- 56 Lin KH, Nalivaika EA, Prachanronarong KL, Yilmaz NK, Schiffer CA. Dengue Protease Substrate Recognition: Binding of the Prime Side. *ACS Infect Dis*. 2016;2:734–743. <https://doi.org/10.1021/acsinfectdis.6b00131>.
- 57 Lin K-H, Ali A, Rusere L, Soumana DI, Kurt Yilmaz N, Schiffer CA. Dengue Virus NS2B/NS3 Protease Inhibitors Exploiting the Prime Side. *J Virol*. 2017;91:1–10. <https://doi.org/10.1128/jvi.00045-17>.
- 58 Qian Z, Liu T, Liu YY, et al. Efficient delivery of cyclic peptides into mammalian cells with short sequence motifs. *ACS Chem Biol*. 2013;8:423–431. <https://doi.org/10.1021/cb3005275>.

- 59 Qian Z, Larochele JR, Jiang B, et al. Early endosomal escape of a cyclic cell-penetrating peptide allows effective cytosolic cargo delivery. *Biochemistry*. 2014;53:4034–4046. <https://doi.org/10.1021/bi5004102>.
- 60 Takagi Y, Matsui K, Nobori H, et al. Discovery of novel cyclic peptide inhibitors of dengue virus NS2B-NS3 protease with antiviral activity. *Bioorganic Med Chem Lett*. 2017;27:3586–3590. <https://doi.org/10.1016/j.bmcl.2017.05.027>.
- 61 De La Cruz L, Nguyen THD, Ozawa K, et al. Binding of low molecular weight inhibitors promotes large conformational changes in the dengue virus ns2b-ns3 protease: Fold analysis by pseudocontact shifts. *J Am Chem Soc*. 2011;133:19205–19215. <https://doi.org/10.1021/ja2084355>.
- 62 Johnston PA, Phillips J, Shun TY, et al. HTS identifies novel and specific uncompetitive inhibitors of the two-component NS2B-NS3 proteinase of West Nile virus. *Assay Drug Dev Technol*. 2007;5:737–750. <https://doi.org/10.1089/adt.2007.101>.
- 63 Koh-Stenta X, Joy J, Wang SF, et al. Identification of covalent active site inhibitors of dengue virus protease. *Drug Des Devel Ther*. 2015;9:6389–6399. <https://doi.org/10.2147/DDDT.S94207>.
- 64 Kiat TS, Phippen R, Yusof R, Ibrahim H, Khalid N, Rahman NA. Inhibitory activity of cyclohexenyl chalcone derivatives and flavonoids of fingerroot, *Boesenbergia rotunda* (L.), towards dengue-2 virus NS3 protease. *Bioorganic Med Chem Lett*. 2006;16:3337–3340. <https://doi.org/10.1016/j.bmcl.2005.12.075>.
- 65 Yildiz M, Ghosh S, Bell JA, Sherman W, Hardy JA. Allosteric inhibition of the NS2B-NS3 protease from dengue virus. *ACS Chem Biol*. 2013;8:2744–2752. <https://doi.org/10.1021/cb400612h>.
- 66 Mukhametov A, Newhouse EI, Aziz NA, Saito JA, Alam M. Allosteric pocket of the dengue virus (serotype 2) NS2B/NS3 protease: In silico ligand screening and molecular dynamics studies of inhibition. *J Mol Graph Model*. 2014;52:103–113. <https://doi.org/10.1016/j.jmgm.2014.06.008>.
- 67 De Sousa LRF, Wu H, Nebo L, et al. Flavonoids as noncompetitive inhibitors of Dengue virus NS2B-NS3 protease: Inhibition kinetics and docking studies. *Bioorganic Med Chem*. 2015;23:466–470. <https://doi.org/10.1016/j.bmc.2014.12.015>.
- 68 Ghosh I, Talukdar P. Molecular docking and pharmacokinetics study for selected leaf phytochemicals from *Carica papaya* Linn. against dengue virus protein, NS2B/NS3 protease. *World Sci News*. 2019;124:264–78.
- 69 Dwivedi VD, Bharadwaj S, Afroz S, et al. Anti-dengue infectivity evaluation of bioflavonoid from *Azadirachta indica* by dengue virus serine protease inhibition. *J Biomol Struct Dyn*. 2020;1102. <https://doi.org/10.1080/07391102.2020.1734485>.
- 70 Farooq MU, Munir B, Naees S, et al. Exploration of *Carica papaya* bioactive compounds as potential inhibitors of dengue NS2B, NS3 and NS5 protease. *Pak J Pharm Sci*. 2020;33:355–360. <https://doi.org/10.36721/PJPS.2020.33.1.SUP.355-360.1>.
- 71 Lim WZ, Cheng PG, Abdulrahman AY, Teoh TC. The identification of active compounds in *Ganoderma lucidum* var. *antler* extract inhibiting dengue virus serine protease and its computational studies. *J Biomol Struct Dyn*. 2020;38:4273–4288. <https://doi.org/10.1080/07391102.2019.1678523>.
- 72 Dwivedi VD, Tripathi IP, Mishra SK. In silico evaluation of inhibitory potential of triterpenoids from *azadirachta indica* against therapeutic target of dengue virus, NS2B-NS3 protease. *J Vector Borne Dis*. 2016;53:156–161.
- 73 Chen S, Xu J, Liu C, et al. Genome sequence of the model medicinal mushroom *Ganoderma lucidum*. *Nat Commun*. 2012;3:1–9. <https://doi.org/10.1038/ncomms1923>.
- 74 El-Mekkawy S, Meselhy MR, Nakamura N, et al. Anti-HIV-1 and anti-HIV-1-protease substances from *Ganoderma lucidum*. *Phytochemistry*. 1998;49:1651–1657. [https://doi.org/10.1016/S0031-9422\(98\)00254-4](https://doi.org/10.1016/S0031-9422(98)00254-4).
- 75 Bharadwaj S, Lee KE, Dwivedi VD, et al. Discovery of *Ganoderma lucidum* triterpenoids as potential inhibitors against Dengue virus NS2B-NS3 protease. *Sci Rep*. 2019;9:1–12. <https://doi.org/10.1038/s41598-019-55723-5>.
- 76 Balasubramanian A, Manzano M, Teramoto T, Pilankatta R, Padmanabhan R. High-throughput screening for the identification of small-molecule inhibitors of the flaviviral protease. *Antiviral Res*. 2016;134:6–16. <https://doi.org/10.1016/j.antiviral.2016.08.014>.
- 77 Anand P, Kunnumakkara AB, Newman RA, Aggarwal BB. Bioavailability of curcumin: Problems and promises. *Mol Pharm*. 2007;4:807–818. <https://doi.org/10.1021/mp700113r>.
- 78 Wang YJ, Pan MH, Cheng AL, et al. Stability of curcumin in buffer solutions and characterization of its degradation products. *J Pharm Biomed Anal*. 1997;15:1867–1876. [https://doi.org/10.1016/S0731-7085\(96\)02024-9](https://doi.org/10.1016/S0731-7085(96)02024-9).
- 79 Balasubramanian A, Pilankatta R, Teramoto T, et al. Inhibition of dengue virus by curcuminoids. *Antiviral Res*. November 2018;2019:71–78. <https://doi.org/10.1016/j.antiviral.2018.12.002>.
- 80 Zamri A, Teruna HY, Rahmawati EN, Frimayanti N, Ikhtiarudin I. Synthesis and in silico studies of a benzenesulfonyl curcumin analogue as a new anti dengue virus type 2 (DENV2) NS2B/NS3. *Indones J Pharm*. 2019;30:84–90. https://doi.org/10.14499/indonesianjpharm30iss2_pp84.
- 81 Lee JC, Chang FR, Chen SR, et al. Anti-dengue virus constituents from Formosan zoanthid *Palythoa mutuki*. *Mar Drugs*. 2016;14:1–10. <https://doi.org/10.3390/md14080151>.
- 82 Tataringa G, Spac A, Sathyamurthy B, Zbancnic AM. In silico studies on some dengue viral proteins with selected *Allium cepa* oil constituents from Romanian source. *Farmacia*. 2020;68:48–55. <https://doi.org/10.31925/farmacia.2020.1.8>.
- 83 Wu H, Bock S, Snitko M, et al. Novel dengue virus NS2B/NS3 protease inhibitors. *Antimicrob Agents Chemother*. 2015;59:1100–1109. <https://doi.org/10.1128/AAC.03543-14>.
- 84 Raut R, Beesetti H, Tyagi P, et al. A small molecule inhibitor of dengue virus type 2 protease inhibits the replication of all four dengue virus serotypes in cell culture. *Virology*. 2015;12:1–7. <https://doi.org/10.1186/s12985-015-0248-x>.
- 85 Li L, Basavannacharya C, Chan KWK, Shang L, Vasudevan SG, Yin Z. Structure-guided discovery of a novel non-peptide inhibitor of dengue virus NS2B-NS3 protease. *Chem Biol Drug Des*. 2015;86:255–264. <https://doi.org/10.1111/cbdd.12500>.
- 86 Timiri AK, Subasri S, Keshewani M, et al. Synthesis and molecular modelling studies of novel sulphonamide derivatives as dengue virus 2 protease inhibitors. *Bioorg Chem*. 2015;74–82. <https://doi.org/10.1016/j.bioorg.2015.07.005>.
- 87 Pelliccia S, Wu YH, Coluccia A, et al. Inhibition of dengue virus replication by novel inhibitors of RNA-dependent RNA polymerase and protease activities. *J Enzyme Inhib Med Chem*. 2017;32:1091–1101. <https://doi.org/10.1080/14756366.2017.1355791>.
- 88 Hariono M, Choi SB, Roslim RF, et al. Thioguanine-based DENV-2 NS2B/NS3 protease inhibitors: Virtual screening, synthesis, biological evaluation and molecular modelling. *PLoS ONE*. 2019;14:1–21. <https://doi.org/10.1371/journal.pone.0210869>.
- 89 Bhowmick S, Alissa SA, Wabaidur SM, Chikhale RV, Islam MA. Structure-guided screening of chemical database to identify NS3-NS2B inhibitors for effective therapeutic application in dengue infection. *J Mol Recognit*. 2020;33:1–18. <https://doi.org/10.1002/jmr.2838>.
- 90 Gan CS, Lee YK, Heh CH, Rahman NA, Yusof R, Othman S. The synthetic molecules YK51 and YK73 attenuate replication of dengue virus serotype 2. *Trop Biomed*. 2017;34:270–283.
- 91 El-Subbagh HI, Abu-Zaid SM, Mahran MA, Badria FA, Al-Obaid AM. Synthesis and biological evaluation of certain α , β -unsaturated ketones and their corresponding fused pyridines as antiviral and cytotoxic agents. *J Med Chem*. 2000;43:2915–2921. <https://doi.org/10.1021/jm000038m>.
- 92 Cheng D, Valente S, Castellano S, et al. Novel 3,5-bis(bromohydroxybenzylidene) piperidin-4-ones as coactivator-associated arginine methyltransferase 1 inhibitors: Enzyme selectivity and cellular activity. *J Med Chem*. 2011;54:4928–4932. <https://doi.org/10.1021/jm200453n>.
- 93 Kálai T, Kuppusamy ML, Balog M, et al. Synthesis of N-substituted 3,5-bis(arylidene)-4-piperidones with high antitumor and antioxidant activity. *J Med Chem*. 2011;54:5414–5421. <https://doi.org/10.1021/jm200353f>.
- 94 Basiri A, Xiao M, McCarthy A, Dutta D, Byrareddy SN, Conda-Sheridan M. Design and synthesis of new piperidone grafted acetylcholinesterase inhibitors. *Bioorganic Med Chem Lett*. 2017;27:228–231. <https://doi.org/10.1016/j.bmcl.2016.11.065>.
- 95 Frimayanti N, Chee CF, Zain SM, Rahman NA. Design of new competitive dengue NS2B/NS3 protease inhibitors—a computational approach. *Int J Mol Sci*. 2011;12:1089–1100. <https://doi.org/10.3390/ijms12021089>.
- 96 Osman H, Idris NH, Kamarulzaman EE, Wahab HA, Hassan MZ. 3,5-Bis(arylidene)-4-piperidones as potential dengue protease inhibitors. *Acta Pharm Sin B*. 2017;7:479–484. <https://doi.org/10.1016/j.apsb.2017.04.009>.
- 97 Padmapriya P, Gracy Fathima S, Ramanathan G, et al. Development of antiviral inhibitor against dengue 2 targeting NS3 protein: In vitro and in silico significant studies. *Acta Trop*. 2018;188:1–8. <https://doi.org/10.1016/j.actatropica.2018.08.022>.
- 98 Kühl N, Graf D, Bock J, Behnam MAM, Leuthold MM, Klein CD. A New Class of Dengue and West Nile Virus Protease Inhibitors with Submicromolar Activity in Reporter Gene DENV-2 Protease and Viral Replication Assays. *J Med Chem*. 2020;63:8179–8197. <https://doi.org/10.1021/acs.jmedchem.0c00413>.
- 99 Zhou GC, Weng Z, Shao X, et al. Discovery and SAR studies of methionine-proline amides as dengue virus NS2B-NS3 protease inhibitors. *Bioorganic Med Chem Lett*. 2013;23:6549–6554. <https://doi.org/10.1016/j.bmcl.2013.10.071>.
- 100 Weng Z, Shao X, Graf D, et al. Identification of fused bicyclic derivatives of pyrrolidine and imidazolidinone as dengue virus-2 NS2B-NS3 protease inhibitors. *Eur J Med Chem*. December 2015;2017:751–759. <https://doi.org/10.1016/j.ejmech.2016.09.063>.
- 101 Knehans T, Schüller A, Doan DN, et al. Structure-guided fragment-based in silico drug design of dengue protease inhibitors. *J Comput Aided Mol Des*. 2011;25:263–274. <https://doi.org/10.1007/s10822-011-9418-0>.
- 102 Beyler SA, Zaneveld LJD. Antifertility activity of systemically administered proteinase (acrosin) inhibitors. *Contraception*. 1982;26:137–146. [https://doi.org/10.1016/0010-7824\(82\)90082-8](https://doi.org/10.1016/0010-7824(82)90082-8).
- 103 Bartolini M, Cavrini V, Andrisano V. Characterization of reversible and pseudo-irreversible acetylcholinesterase inhibitors by means of an immobilized enzyme reactor. *J Chromatogr A*. 2007;1144(1):102–110. <https://doi.org/10.1016/j.chroma.2006.11.029>.
- 104 Sundermann TR, Benzin CV, Dražić T, Klein CD. Synthesis and structure-activity relationships of small-molecular di-basic esters, amides and carbamates as flaviviral protease inhibitors. *Eur J Med Chem*. 2019;176:187–194. <https://doi.org/10.1016/j.ejmech.2019.05.025>.
- 105 Chu JHH, Lee RCH, Ang MJY, et al. Antiviral activities of 15 dengue NS2B-NS3 protease inhibitors using a human cell-based viral quantification assay. *Antiviral Res*. 2015;118:68–74. <https://doi.org/10.1016/j.antiviral.2015.03.010>.
- 106 Bhakat S, Delang L, Kaptein S, Neyts J, Leyssen P, Jayaprakash V. Reaching beyond HIV/HCV: Nelfinavir as a potential starting point for broad-spectrum protease inhibitors against dengue and chikungunya virus. *RSC Adv*. 2015;5:85938–85949. <https://doi.org/10.1039/c5ra14469h>.
- 107 AN, Ming; CHANG, Zhen; GAO, Lei; LI, Mei; CAO G. Determination of Four Related Substances in Poliresulen Solution by HPLC. *Chinese J Pharm Anal*. 2004;24:536–37.

- 108 Wu DW, Mao F, Ye Y, et al. Policresulen, a novel NS2B/NS3 protease inhibitor, effectively inhibits the replication of DENV2 virus in BHK-21 cells. *Acta Pharmacol Sin.* 2015;36:1126–1136. <https://doi.org/10.1038/aps.2015.56>.
- 109 Li Z, Brecher M, Deng YQ, et al. Existing drugs as broad-spectrum and potent inhibitors for Zika virus by targeting NS2B-NS3 interaction. *Cell Res.* 2017;27(8): 1046–1064. <https://doi.org/10.1038/cr.2017.88>.
- 110 Li Z, Zhang J, Li H. Flavivirus NS2B/NS3 Protease: Structure, Function, and Inhibition. Elsevier Inc.; 2017. doi:10.1016/B978-0-12-809712-0.00007-1.
- 111 Li Z, Sakamuru S, Huang R, et al. Erythrosin B is a potent and broad-spectrum orthosteric inhibitor of the flavivirus NS2B-NS3 protease. *Antiviral Res.* December 2017;2018:217–225. <https://doi.org/10.1016/j.antiviral.2017.12.018>.
- 112 Viswanathan U, Tomlinson SM, Fonner JM, Mock SA, Watowich SJ. Identification of a Novel Inhibitor of Dengue Virus Protease through Use of a Virtual Screening Drug Discovery Web Portal. *J Chem Inf Model.* 2014;54:2816–2825. <https://doi.org/10.1021/ci500531r>.